Design and Techno-Economic Analysis of Agrivoltaic System In the Context of Bangladesh

By

Zihan Rejwana
22361001

A thesis submitted to the Department of Electrical & Electronic Engineering in partial fulfillment of the requirements for the degree of
Master of Science in Electrical & Electronic Engineering

Department of Electrical & Electronic Engineering
BRAC University
January 2026

Declaration

It is hereby declared that

1. The thesis submitted is my own original work while completing degree at BRAC University.
2. The thesis does not contain material previously published or written by a third party, except where this is appropriately cited through full and accurate referencing.
3. The thesis does not contain material which has been accepted, or submitted, for any other degree or diploma at a university or other institution.
4. I have acknowledged all main sources of help.

Student's Full Name & Signature:

Zihan Rejwana
22361001

Approval

Approval

The thesis titled "Design and Techno-Economic Analysis of Agrivoltaic System In the Context of Bangladesh" submitted by

1. Zihan Rejwana (22361001)

of Fall 2025 has been accepted as satisfactory in partial fulfillment of the requirement for the degree of Master of Science in EEE on January 7, 2026.

Examining Committee:

Supervisor:
(Chair of the committee)

Dr. Md. Mosaddequr Rahman
Professor, Department of EEE
BRAC University

Internal Examiner:
(Member)

14.01.2026
Dr. Nahid Akhter Jahan
Associate Professor, Department of EEE
BRAC University

External Expert Examiner:
(Member)

14.01.26
Dr. Taskin Jamal
Associate Professor, Department of EEE
Ahsanullah University of Science & Technology

Departmental Head:
(Ex. Officio)

14.01.26
Dr. Md. Mosaddequr Rahman
Professor, Department of EEE
BRAC University

Ethics Statement

This research was conducted in accordance with accepted academic and research ethics standards. The study is based entirely on analytical modeling, simulation, and secondary data obtained from published literature and publicly available sources. No human participants, animal subjects, or confidential data were involved. All sources of information have been properly cited, and due care has been taken to present results objectively, without data fabrication, falsification, or misrepresentation. The author declares that this work is original, the similarity index below 30% and has not been submitted elsewhere for academic credit.

Abstract/ Executive Summary

Agrivoltaic systems provide a viable approach to addressing land-use competition between agriculture and solar energy, particularly in Bangladesh. This thesis aims to design and evaluate an agrivoltaic system for a representative site in Bangladesh by integrating technical performance analysis with economic feasibility, while limiting crop yield reduction to a maximum of 25%. A techno-economic assessment is conducted using solar irradiation analysis, geometric shadow modeling, and three-dimensional (3D) shading simulations. The impacts of key design parameters, including panel tilt, mounting height, inter-row spacing, and inter-panel gap, are systematically evaluated. A fixed-tilt photovoltaic system with tilt equal to the site latitude is analyzed and compared with a flat installation, considering seasonal weather conditions. Geometric shadow calculations are validated against 3D SketchUp simulations. Results indicate that the latitude-tilted configuration captures approximately 11% higher annual solar energy than a flat system. Shadow length exhibits a U-shaped seasonal trend, with maximum shading during the winter months (October–February) and increased variation at higher panel elevations. The geometric and 3D shading models show close agreement, with deviations within 10%. Increasing inter-row spacing reduces ground coverage ratio and energy yield while improving crop yield, whereas overall land equivalent ratio remains nearly unchanged for two-crop systems. Simulation outcomes show that the Land Equivalent Ratio (LER) spans from 1.14 to 1.27 across all configurations. Of the 18 design options analyzed, 14 achieve LER values between 1.20 and 1.27, which can be considered the optimal range, reflecting consistently high land-use efficiency for most of the proposed agrivoltaic layouts. Economic analysis reveals that energy revenue contributes over 90% of total profit. An optimal design is recommended with a ground coverage ratio close to 0.30 and inter-row spacing of 100–300 cm to maintain profit loss within 25%.

Keywords: Agrivoltaic, Incident Energy, Crop Yield, Ground Coverage Ratio, Land Equivalent Ratio, Return on Investment.

Dedication

I dedicate this thesis to my beloved parents, whose unconditional love, support, and prayers have been my constant source of strength throughout this journey. I am also deeply grateful to my supervisor, Prof. Dr. Md. Mosaddequr Rahman, for his invaluable guidance, encouragement, and mentorship, which have been instrumental in shaping this work.

Table of Contents

List of Tables

List of Figures

List of Acronyms

APV	Agri Photovoltaic
AVS	Agrivoltaic System
GCR	Ground Coverage Ratio
LER	Land Equivalent Ratio
ROI	Return on Investment
CAPEX	Capital Expenditure
OPEX	Operating Expenditure

Chapter 1

Introduction

1.1 Background

Agrivoltaic (AV), a comparably new term in the field of energy production, a process where we can grow crops simultaneously along with energy with the help of photovoltaic (PV) module structured above the farmland. The process is highly applicable for the country with lack of free land, and which is far behind meeting the energy demand. Here the PV module not only produces energy but also prevents water from the field from evaporating thus saving water and preventing the grain from drying out during excess heat of summer [1-2]. This type of clean energy is highly needed because conventional energy production methods produce 475g of CO_2 to produce 1KWh of electricity which is highly contaminated for the environments and the surrounding livings whereas energy generated from solar does not emit any harmful substance as a result we can say it as impactful toward clean world [3].

As an emerging topic agrivoltaic has already been implemented in some of the areas of the world as research purpose or for commercial electricity generation purposes. Currently the world's largest agrivoltaic system (AVS), encompassing around 13 hectares, was developed in the German state of Brandenburg. The idea combines a solar power plant and a crop field to provide both electricity and food [4]. In South Korea they get an 18.7% decrease in the rice yield and in Spain they get a 17% reduction in potato production [5-6]. According to the study [7], installing PV panels in agricultural lands can mitigate the conflict of proper utilization of land by increasing the energy output. Authors claimed that strong financial return can be availed by co-production of crops and electricity in the same land [8]. Study suggested the use of tilt mounted PV panels are beneficial for shade intolerant crops that include rice [9].

The main problem addressed in this study is the competition for land between solar energy installations and agriculture, especially in densely populated developing countries. While agrivoltaic systems have shown promise in Europe and North America, their design, performance, and applicability in the context of South Asia—especially Bangladesh—remain largely unstudied.

Improper design of PV panel layout in agrivoltaic systems can lead to:

- Excessive shading on crops, reducing photosynthesis and agricultural yield [10].
- Reduced PV efficiency due to non-optimal tilt and orientation.
- Poor economic performance if neither energy nor food output is optimized [11].

Furthermore, there is a lack of localized shadow analysis models that consider Bangladesh's unique solar geometry, crop cycles (especially rice), and land-use priorities. Therefore, this study aims to provide a geometrical and conceptual framework for evaluating and designing such system.

1.2 Literature Review

Agrivoltaics refers to the simultaneous production of agricultural crops and solar electricity on the same land area, offering a potential solution to land-use conflicts between food production and renewable energy expansion. The concept was first introduced by Goetzberger and Zastrow in 1982, who proposed a photovoltaic power plant design that allows continued agricultural use beneath PV collectors and derived analytical relationships to estimate light transmission to the ground under solar arrays [12]. Since then, AVS has been extensively studied to enhance overall land productivity.

Early modeling work by Dupraz et al. (2011) quantified light availability at crop level under PV arrays and integrated crop growth models to estimate yield under partial shading. Their results demonstrated that agrivoltaic systems could increase overall land productivity by 35% to 73%, depending on PV density [13]. Subsequent experimental studies by Marrou et al. (2013) showed that crop growth rates under PV-induced shading were only moderately affected and that limited adjustments in agricultural practices were sufficient when transitioning from open-field farming to AV systems [14]. Further economic assessments, such as those by Dinesh et al. (2016), highlighted the strong financial potential of agrivoltaics, reporting more than a 30% increase in farm value compared to conventional agriculture when shade-tolerant crops were used [15].

Globally, agrivoltaic deployment has expanded rapidly. By 2020, approximately 2,200 systems were installed worldwide, with Japan leading the adoption through nearly 2,000 agrivoltaic farms and an installed capacity of about 2.8 GWp, contributing roughly 0.8% of national PV output [16]. Similar developments have been reported in Europe, where innovative designs such as vertical bifacial PV systems with wide row spacing have been successfully implemented for crops including potatoes, hay, and silage in Germany and Austria [17].

Numerous crop-specific studies conducted in Asia and Europe indicate that agrivoltaic performance is highly dependent on crop type and system design. Investigations in India and Malaysia on crops such as aloe vera, spinach, and java tea demonstrated yield improvements under controlled shading, alongside reductions in PV module temperature and corresponding increases in energy yield [18–24]. Research on shade-intolerant crops such as corn revealed that moderate shading can maintain or even enhance yields at lower PV densities, while excessive shading leads to production losses [25].

Land-use efficiency in agrivoltaic systems is commonly assessed using the Land Equivalent Ratio (LER), which combines relative energy and crop yields. Reported LER values typically range from 1.2 to 1.6, corresponding to a 60–70% improvement in land productivity compared to separate PV and agricultural systems [13, 26]. Several studies have shown that agrivoltaic systems also improve water-use efficiency by reducing evapotranspiration and heat stress, particularly in dry or drought-prone regions [13, 14, and 27]. Field experiments on lettuce, berries, and grapes further demonstrated that shading could reduce thermal stress without significantly affecting plant temperature or air circulation, leading to yield stability or even increases for certain crops [13, 14, 28, 29].

Recent work has emphasized the importance of geometric design parameters such as ground coverage ratio (GCR), inter-row spacing, and panel height. Studies from Sweden and Germany showed that excessive PV density or narrow row spacing can significantly reduce crop yields, even when LER remains high, indicating that LER alone is insufficient for optimal system design [30, 31]. Crop-specific optimization is therefore essential to balance energy generation and agricultural productivity. Economic analyses, including Monte Carlo–based assessments for apple cultivation in Hungary, confirmed the financial viability of AV systems while highlighting electricity pricing and financing conditions as dominant factors [20].

Agrivoltaics has also been evaluated for staple crops such as rice, where yield reductions of approximately 20–25% were reported under shaded conditions, yet overall economic returns remained substantially higher than mono-cropping due to energy revenue [22]. Meta-analyses and microclimate studies further revealed that shading effects vary seasonally: increased shading may reduce productivity during low-radiation periods, while providing benefits during hot seasons by mitigating heat and water stress [24,32].

Finally, several European countries have introduced regulatory frameworks to ensure that agrivoltaic deployment does not compromise agricultural productivity. Regulations in Italy, France, and Spain specify limits on PV coverage and allowable crop yield reductions, reflecting a policy-driven effort to balance food security and renewable energy expansion [23]. Collectively, these studies confirm that well-designed agrivoltaic systems can substantially improve land-use efficiency, if system geometry, crop selection, and local climatic conditions are carefully considered. Table 1.1 summarizes some of the key findings for agrivoltaics systems existed in Bangladesh, India and global summary. From the literature it is found that LER for rice crops is higher than the 1 and GCR varies in between 0.2-0.5.

Table 1.1.: Agrivoltaic work in Bangladesh, India and Global Summary

Region / Study	Crops Studied	PV Configuration	Observed Yield / Effect	LER	GCR	Payback / Economics	Reference
Bangladesh – Chuadanga agrivoltaic case	Multiple field crops under panels	Ground-mounted PV	No significant reduction in crop yield;	Not specified	Not specified	Not specified	[72]
Bangladesh – National agrivoltaic potential	Not specific crop	Agrivoltaics conceptual land use	103% crop yield	~1.86 (combined land use)	Not specified		[73]
India – SRM Institute agrivoltaic comparison	Not specific crop (experimental dual use)	Rooftop agrivoltaic + 4.3 kW agrivoltaic system	12.7% higher power vs rooftop	1.85	Not specified	payback ~6–7 years	[74]
India – ICAR-CAZRI, Jodhpur project	Mung bean, moth bean, cluster bean, chickpea, cumin, isabgol	Field PV rows with inter-row crop zones	Yield reductions 4–11% vs control (varied by crop)	~1.42–1.62	~0.49 land under PV used for crop growth (interspaces)	Irrigated AVS PBP ~7.47 years; rainfed ~8.11 years;	[75]
Global review with specific agrivoltaic crop focus	Rice (modelled)	Bifacial agrivoltaic systems	Rice yield reduction limited to ~18% at GCR 30%	>1 (greater combined productivity)	20–50% GCR evaluated	Payback ~11–12 years	[76]
Odisha agrivoltaic dual use in broader context	Various crops	Side-by-side PV with crops	Dual agricultural and energy yields shown	1.41 combined LER for AV in India	Not specified	Revenue from solar and crop yields; payback ~8 years	[77]

1.3 Objective of the Study

The primary goal of this thesis is to design analysis of agrivoltaic system for a land of Bangladesh, considering different technical & economic factors. The specific objectives are:

- To analyze solar geometry and shadow behavior over different seasons.
- To evaluate the impact of panel height, tilt, inter-panel and inter-row spacing on shading
- To study the relationship between Ground Coverage Ratio (GCR), relative crop yield, and energy output.
- To estimate theoretical PV energy yield under different panel configurations.
- To calculate the land-equivalent ratio (LER) for different designs.
- To estimate the economic aspects of different designs

1.4 Scope of the Study

The scope of this research is focused on:

- Computation of solar irradiation and potential energy yield for the selected site.
- Geometric determination of inter-panel and inter-row spacing, along with the assessment of panel height impact, leading to detailed shadow analysis.
- Performance evaluation of the proposed agrivoltaic system based on different design parameters.
- Techno-economic assessment to determine system feasibility and overall cost-effectiveness.

1.5 Thesis Organization

This thesis is organized into five chapters as follows:

- **Chapter 1: Introduction** – Presents the motivation, background, research gap, objectives, and scope.
- **Chapter 2: Theoretical Background** – Reviews the key concepts of solar PV systems, shading, agronomic impacts of shading, and land use metrics like LER and GCR.
- **Chapter 3: Methodology** – Describes the geometrical modeling approach, system design assumptions, and equations used for analysis.
- **Chapter 4: Result Analysis and Discussion** – Analyzes shadow patterns, GCR-yield trade-offs, and theoretical energy output.
- **Chapter 5: Conclusion and Future Works** – Summarizes findings, implications, and provides suggestions for future research or implementation.

:

Chapter 2

Theoretical Background

2.1 Solar Irradiation Calculation

The total incident solar energy can be determined by applying the following equation (2.1) [33]

$$E_{inc} = A \int_{T_{SR}}^{T_{SS}} I_{inc} dt \qquad (2.1)$$

where *A* denotes the panel's area, and I_{inc} denotes incident solar energy. T_{SS} and T_{SR} are used to denote the sunrise and sunset times. The beam solar irradiance is calculated by using equation (2.2) [33].

$$I = \frac{I_{inc}}{\cos\delta * \cos\theta} \qquad (2.2)$$

where the angle is formed by incident sunlight and the panel plane is θ, and the declination angle is δ. The solar irradiance is obtained from equation (2.3) [34].

$$I_0 = \frac{I}{(0.7)^{AM^{0.678}}} \qquad (2.3)$$

Here, AM denotes the air mass, and I_0 is the solar irradiance outside the earth's atmosphere, which is 1367 W/m^2. The altitude angle, α of the sun is determined using equation (2.4) [34].

$$\alpha = \sin^{-1}(\sin\delta \sin\gamma + \cos\delta \cos\gamma \cos\omega) \qquad (2.4)$$

The latitude angle is represented by γ, ω is the hour angle and the angle of declination is δ which is calculated by using the equation (2.5) [34].

$$\delta = 23.45° \sin\{\frac{360}{365}(n + 284)\} \qquad (2.5)$$

where n is the number of days of the year. The hour angle is calculated by using the equation (2.6) [35].

$$\omega = \omega_S - 15\,(t - T_{SR}) \qquad (2.6)$$

here, *t* is the time of day expressed in reference to solar midnight [35]. The hour angle at sunrise time, ω_S is calculated by using (2.7),

$$\omega_S = \cos^{-1}(-\tan\gamma \tan\delta) \qquad (2.7)$$

The presence of cloud adversely affects solar energy conversion efficiencies. Cloud can block a significant portion of the sun's incoming radiation from reaching the earth's surface. The next procedure was acquiring the amount of energy on sunny days as well as on cloudy days. Here energy of sunny day refers to the energy that is received on a pure shiny day while having the sun directly overhead and cloudy days' energy refers to 20% of the energy on sunny days [35]. Sets of mathematical equations are provided below:

$$E_{sunny} = \int_{T_{SR}}^{T_{SS}} (I sin\alpha + 0.2I)\, dx \qquad (2.8)$$

$$E_{Cloudy} = \int_{T_{SR}}^{T_{SS}} 0.2I\, dx \qquad (2.9)$$

Next approach was to find the approximate number of sunny days and cloudy days by using the subsequent equations:

$$E_{Direct} = x * E_{Sunny} + y * E_{Cloudy} \qquad (2.10)$$

$$x + y = Total\ Days_{particular\ month} \qquad (2.11)$$

While using the following set of equations we finally figured out the number of sunny and cloudy days.

2.2 Agrivoltaic System Defining Parameters

Agrivoltaic systems offer a transformative solution to the competing land demands of food and energy production. By integrating photovoltaic systems with agriculture on the same land area, agrivoltaics supports sustainable land use—particularly critical for densely populated and agriculture-dependent countries like Bangladesh. This chapter discusses the theoretical underpinnings of agrivoltaic systems.

The fundamental idea of agrivoltaics is to install solar PV modules at a certain height and spacing to allow sufficient sunlight to reach the crops below, thereby sharing solar radiation between the two production systems. Instead of competing, the agricultural and energy sectors cooperate to improve the Land Equivalent Ratio (LER) and maximize the overall efficiency of land use [36]. This is particularly important in countries like Bangladesh, where high population density and limited cultivable land put pressure on resource allocation.

Agrivoltaic systems can vary in design depending on the landscape, crop type, and energy goals. The main configurations include:

- *Static Agrivoltaics*: Panels are fixed at a certain tilt and orientation. These systems are simple and cost-effective but may not optimize sunlight distribution over time.
- *Dynamic or Tracking Systems*: These systems use solar trackers to follow the sun's path. While they improve energy yield, they require more complex control systems and can affect the light availability for crops unpredictably [37].
- *Elevated or Vertical Agrivoltaics*: Panels are installed at higher elevations (e.g., 2.5 to 4 meters) or vertically, allowing for uninterrupted agricultural operations (e.g., plowing, harvesting) underneath. Vertical bifacial PV panels are also gaining attention for perimeter installations or narrow fields [38].

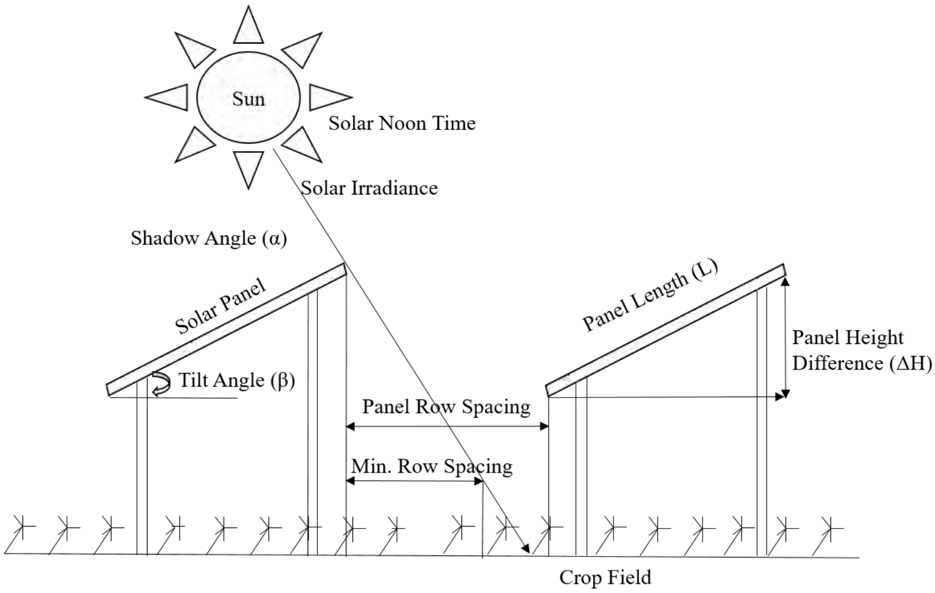

Fig. 2.1 Two-dimensional view of inter-row spacing of adjacent solar panels.

From Fig. 2.1, two-dimensional view of inter row spacing and different angles depends on it can be observed. The effective row spacing between the panels are decided by,

- Panel Tilt (β)
- Panel length (L)
- Height difference (H)
- Shadow angle (α)

2.2.1 Land Equivalent Ratio (LER)

The Land Equivalent Ratio (LER) is a key metric used to assess the efficiency of land use in agrivoltaic systems. It is defined as the ratio of the combined area required by separate monoculture systems (one for agriculture and one for photovoltaic energy production) to the area required by a combined agrivoltaic system to produce the same agricultural and energy output. Mathematically, LER is given by:

$$LER = \frac{Y_{agri,AV}}{Y_{agri,mono}} + \frac{Y_{PV,AV}}{Y_{PV,mono}} \tag{2.12}$$

where $Y_{agri,AV}$ and $Y_{PV,AV}$ are the agricultural and PV yields under the agrivoltaic system, and $Y_{agri,mono}$ and $Y_{PV,mono}$ are the yields under monoculture conditions [39].

An LER greater than 1 indicates that the agrivoltaic system uses land more efficiently than separate, single-use systems. For example, Dupraz et al. [13] reported that an LER of up to 1.7 could be achieved under optimized agrivoltaic configurations, meaning 70% more land productivity. LER is particularly valuable in densely populated and land-scarce countries like Bangladesh, where maximizing land utility is critical. However, achieving a high LER depends on various factors, including crop type, PV system design, GCR, and climatic conditions [10].

2.2.2 Ground Coverage Ratio (GCR)

The Ground Coverage Ratio (GCR) is defined as:

$$GCR = \frac{Area\ Covered\ by\ PV\ Panels}{Total\ Land\ Area} \tag{2.13}$$

A low GCR means more light for crops but less energy generation, while a high GCR favors electricity at the expense of photosynthesis. Optimal GCR values vary by crop type and geography. For example, a GCR of 30–40% has been found optimal for rice in semi-humid regions [40].

2.2.3 Impact of Shadow on Solar PV Systems

Shading is one of the most significant factors that adversely affect the performance of solar photovoltaic (PV) systems. Even partial shading on a PV module can result in disproportionate power losses due to the series connection of solar cells within a panel. When a portion of a PV cell is shaded, it restricts the current flow in the entire string, potentially creating hot spots that degrade module performance and reduce lifespan [41].

Shading can arise from nearby structures, vegetation, dust, or even self-shading between rows of PV panels. In agrivoltaic systems, while some shading is intentional to support crop growth, non-optimized shading patterns can severely impact PV energy yield. To minimize shading losses, PV arrays are often equipped with bypass diodes, which allow current to bypass shaded cells or modules. However, this solution does not completely eliminate energy loss [42].

Furthermore, shading effects vary throughout the day and year, governed by the solar position. In fixed-tilt systems, shading can be particularly critical during early morning and late afternoon hours. As a result, accurate shadow analysis and layout design are essential in agrivoltaics to balance light sharing between crops and panels. Modeling tools like PVsyst, Helioscope, and MATLAB-based simulations are often used to assess shading impacts over seasonal periods [43].

Impact of Panel Height and Inter-Panel Gap on Shading

In agrivoltaic system design, panel height and inter-panel gap are critical geometric parameters that influence the shading profile cast on crops and the overall land area utilization. These parameters determine the length, intensity, and duration of shadows throughout the day, directly affecting both solar energy generation and photosynthetic light availability for crops.

Panel Height:

Increasing the mounting height of PV panels reduces the ground-level shading intensity and allows more diffuse sunlight to reach the crop canopy. Higher mounting also promotes better air circulation, potentially improving microclimatic conditions (e.g., humidity and temperature regulation). However, elevated systems are structurally more complex and costlier, especially in areas with high wind loads [44].

Higher installations are particularly useful for accommodating machinery operations, livestock movement, or taller crop varieties. A study by Dinesh and Pearce (2016) showed that increasing panel height can reduce the negative impact on biomass yield for certain crop types under agrivoltaic setups [45].

Inter-Panel Gap:

The spacing between rows of solar panels, also known as inter-row distance, is a primary factor in managing row-to-row shading. A larger inter-panel gap allows for longer periods of direct sunlight to reach crops, especially during low solar elevation angles. The optimal gap depends on the latitude, panel tilt angle, and crop light requirements.

Balancing panel density (Ground Coverage Ratio, GCR) and light availability is essential. Higher GCR may increase energy yield but risks crop productivity due to excessive shading. A simulation-based study by Majumdar and Pasqualetti (2020) emphasized that dynamic optimization of GCR, panel height, and gap can result in a more efficient agrivoltaic design [46].

2.3 Economic Assessment Parameters

CAPEX (Capital Expenditure):

Capital expenditure, also known as CAPEX, represents the initial investment that requires for the initial installation of the solar panels, proper grid integration and other procurement process for the whole system,[47]

$$CAPEX = C_{panel} + C_{site} + C_{install} + C_{grid-connected} \quad (2.14)$$

Here, $CAPEX$ represents the total initial cost for the project. C_{panel} determines the buying costs of the PV panels, C_{site} represents all the initial costs related to land preparation, $C_{install}$ represents all the costs related to PV panels installation including labour costs and lastly, $C_{grid-connected}$ represents expenses related to grid integration.

OPEX (Annual Operating Expenditure):

Another important parameter related to costs is OPEX, also known as Operational Expenditure. This expense is related to all the necessary annual costs to operate and maintain a solar power plant during its lifetime [48].

$$OPEX = C_{O\&M} + C_{insurance} + C_{contingency} \tag{2.15}$$

Here, $OPEX$ accounts for the annual operational expenses. Also $C_{O\&M}$ represents the yearly operational and maintenance cost. The cost for contingency and insurance are defined as $C_{contingency}$ and $C_{insurance}$ insurance expense and emergency operational expense sequentially.

Degradation of Panel Efficiency:

Every installed solar panel faces gradual efficiency reduction during its total lifetime due to aging and other environmental effects. This degradation rate is related to energy yield,[49]

$$\eta = \eta_0 \times (1 - \delta_{deg}) \tag{2.16}$$

Here, η represents yearly panel efficiency degradation. The initial module efficiency or rated output is defined as $\eta_{\mathbf{0}}$ and $\delta_{\boldsymbol{deg}}$ is defined as the annual degradation rate.

Energy Production:

The annual energy production by the solar panels is calculated from the total installed capacity of the PV panels, solar irradiance incorporated with system losses and panel degradation rate [50],

$$E = P_{size} \times H_{PSH} \times (1 - L_{loss}) \times (1 - \delta_{\boldsymbol{deg}}) \tag{2.17}$$

Here, E represents annual energy production by the PV panels and P_{size} denotes as total installed solar system capacity in KWh. Also, H_{PSH} represents as annual peak sun hours and L_{loss} represents performance losses.

Crop and Energy Revenue:

All the revenue generated for the agrivoltaic systems depends on both revenue from crops and electricity generated by the solar panels.

$$Revenue_{energy} = E \times P_{energy} \quad (2.18\text{-a})$$

Here, $Revenue_{\text{energy}}$ represents the revenue generated from the electrical output from the installed PV panels. Electrical output generation is denoted as E and the selling price for the generated electricity is denoted as Penergy .

$$Revenue_{crop} = Y_{crop} \times P_{crop} \quad (2.18\text{-b})$$

Here, $Revenue_{crop}$ denotes all the calculated income from crops, Y_{crop} represents the crop yield which is kg/ha/year and P_{crop} represents the market price of the agrivoltaic crops which are in currency/ kg.

Crop Costs:

Crop costs is solely dependent on all the expenses related to land preparation, labour costing, harvesting and operation [51],

$$C_{crop} = C_{input} + C_{labour} \times C_{harvest} \quad (2.19)$$

Here, C_{crop} represents all the calculated costs for the crop production. Moreover, C_{input} denotes as all the costs related to agrivoltaic system, C_{labour} represents all the costs related to labour and lastly $C_{harvest}$ refers to all the costs related to crop harvesting.

Net Crop Revenue:

Net Crop revenue represents the value of after subtracting all the costs related to crop production from the gross crop income,[52]

$$NR_{crop} = Income_{crop} - C_{crop} \quad (2.20)$$

Here, NR_{crop} represents the net revenue of the crops which is calculated from subtracting C_{crop} which is basically all the costs related to crop from the income of crops which is $Income_{crop}$.

Yearly Cash Flow:

The Yearly Cash Flow denotes as the yearly net financial outcome from the agrivoltaic system for a specific year,[53]

$$CF = Revenue_{energy} + NR_{crop} - OPEX \qquad (2.21)$$

Here, CF refers to yearly net cash flow. Also, $Revenue_{energy}$ is the calculated revenue that has been generated from PV panels and NR_{crop} represents the net revenue of the crops. From both parameters OPEX, which is operation expenditure, will be deducted.

Net Present Value:

Net Present Value also known as NPV profitability of the initial investment during whole project lifetime,[54]

$$NPV = -CAPEX + \sum_{y=1}^{N} \frac{CF}{(1+r)} \qquad (2.22)$$

Discount Rate:

This discount rate refers to effects of both borrowing interest rate and inflation,[55]

$$r = \frac{1+i}{1+\pi} - 1$$

(2.23)

Here, i represent borrowing interest rate and π represent inflation rate.

Cumulative Cash Flow (CumCF) Over Time:

This Cumulative Cash Flow is also known as $CumCF$ defines the whole cash inflows and outflows during project lifetime.[56]

$$CumCF = -CAPEX + \sum_{y=1}^{Y} \frac{CF}{(1+r)} \tag{2.24}$$

Return on Investment (ROI) and Payback:

Return On Investment also represents ROI or Payback is the measurement of profitability of the whole agrivoltaic system related to initial capital investment [57].

$$ROI = \frac{\sum_{y=1}^{N} CF}{CAPEX} \tag{2.25}$$

Here, CF as the yearly cash flow during the project lifetime and $CAPEX$ represents capital expenditure which is the initial investment.

Chapter 3

System Design and Methodology

3.1 Shadow of a vertical Panel from origin

Figure 3.1 shows the shadow components of a Panel of height H at the origin. The sun is altitude (at solar hour angle ω) and in azimuth γ. The shadow length F is found from the equation (3.1) [58]

$$F = \frac{H}{tan\alpha} \tag{3.1}$$

The relation between the sun altitude α, latitude φ, declination angle δ and the hour angle ω, is given by (3.2) [58];

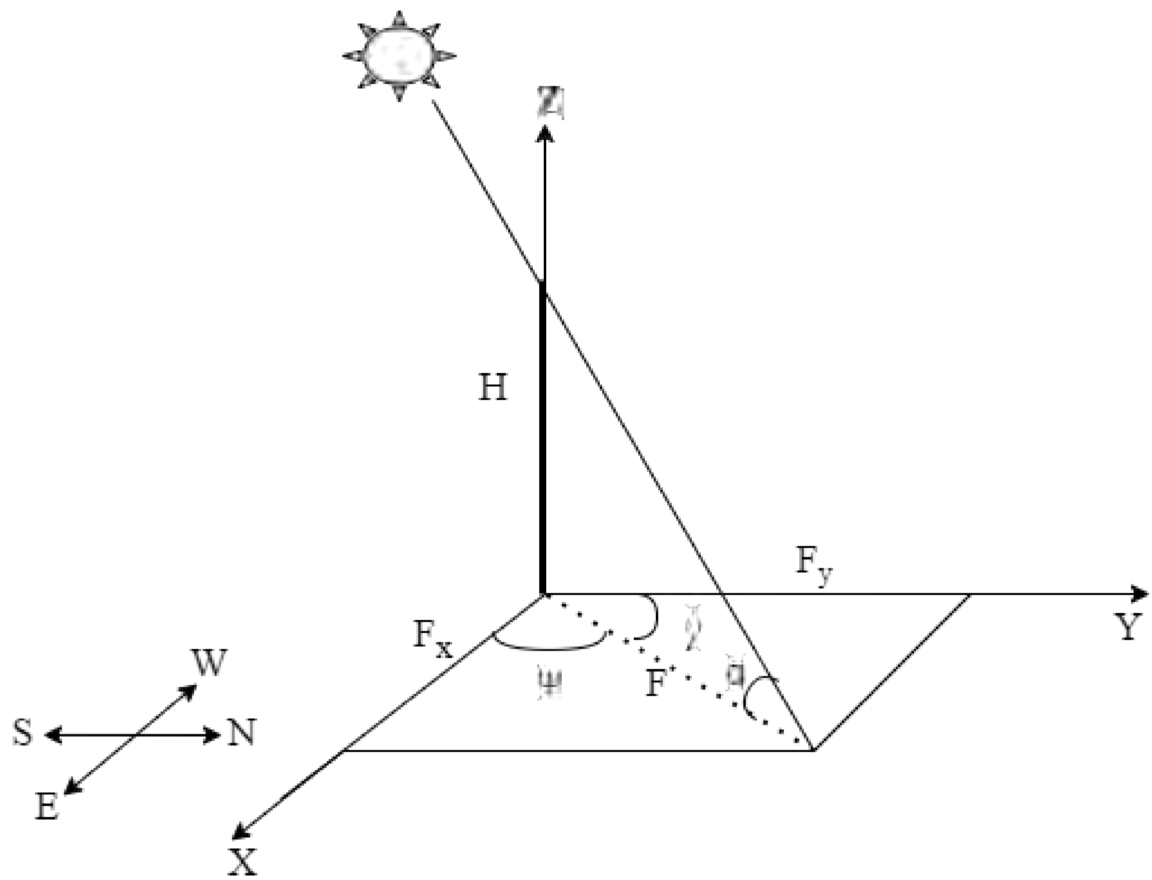

Fig. 3.1. Shadow components of a vertical Panel [58].

$$\sin\alpha = sin\varphi\ sin\delta + cos\varphi\ cos\delta\ cos\omega \qquad (3.2)$$

The east-west shadow component can be found from (3.3) [58]

$$F_X = \frac{H \ \cdot sin\gamma}{tan\alpha} \qquad (3.3)$$

Similarly north-south component is

$$F_Y = \left(\frac{H \ \cdot \cos\gamma}{tan\alpha}\right) \qquad (3.4)$$

3.2 Shadow of an Inclined Panel above the ground

The shadow position theory of the inclined solar collector has been described in Fig. 3.2. The north-south shadow component can be estimated from the Y axis, and the east-west shadow component can be calculated from the X axis in the northern hemisphere, where the origin is O [58]. The length of the shadow can be determined from the values of the X and Y components. *H'* is the height of the installed agri-voltaic system from the ground. Therefore, O'B is the tilted collector's shifted surface, '*A*' is the collector's side edge length, β is the tilt angle from the surface, and *H* is the inclined Panel height from the surface due to the tilt angle. The shadow edge positions C (P_x, P_y) and C' ($P_{x'}$, $P_{y'}$) are caused by the inclined Panel O'M, where OC and OC' from the origin may be obtained from the X-axis and Y-axis components. The shaded length formed by the collector edge has been classified as CC', whereas the unshaded length is OC.

The shadow length usually equals the Y-axis component at solar noon, with the X-axis component closest to the origin. The other edge of the panel has the identical P_y and $P_{y'}$ components, whereas the X-axis component has been shifted right from the origin to the width of the collector. In this study, the OC' length of the shadow has been more closely observed in order to measure the inter-row and inter-panel distance.

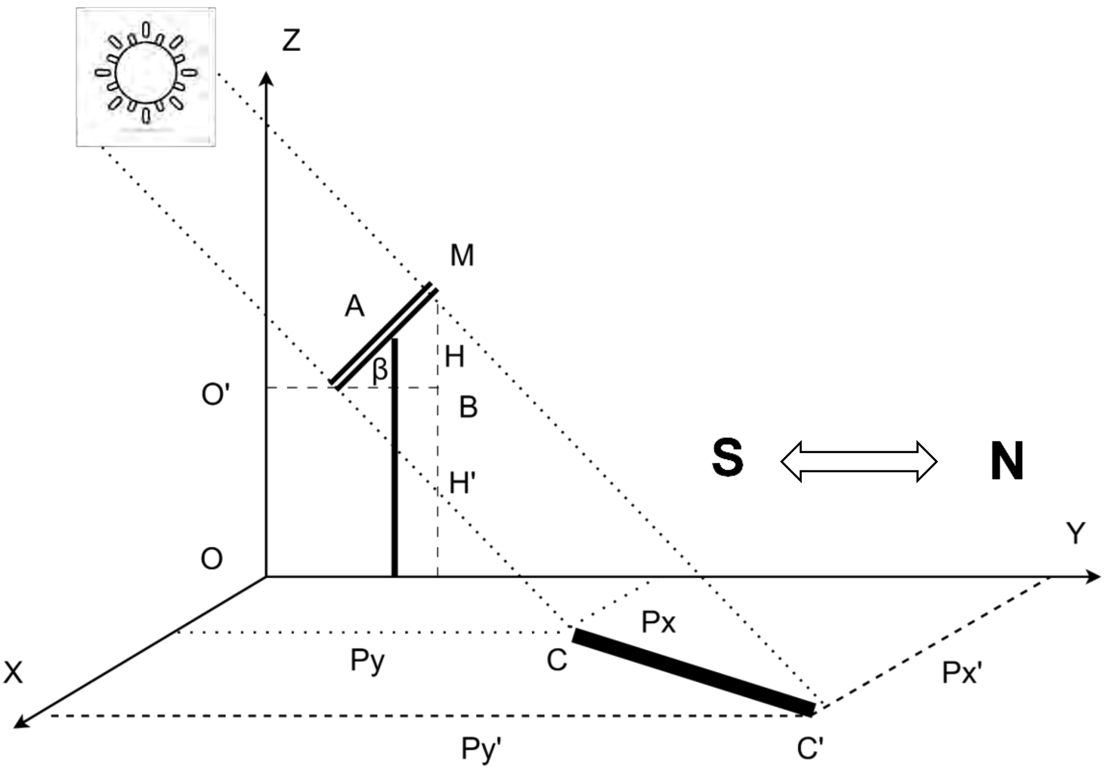

Fig. 3.2. Shadow components of an inclined panel above the origin.

Calculating the height and length of the shadow that any collector projects on nearby objects is part of the basics of shadow analysis.

The east-west and north-south components of the shadow, OC (in the X-axis and Y-axis) can be calculated from these equations,

$$P_X = F_x = \frac{H \cdot sin\gamma}{tan\alpha} \qquad (3.5)$$

$$P_Y = F_y = \left(\frac{H \cdot \cos\gamma}{tan\alpha}\right) \qquad (3.6)$$

Where, A is the length of the inclined collector, H' is the height from the ground surface, O'M, inclined angle towards south direction has been denoted by β and the solar azimuth is γ .

The inclined Panel height, H can be found from here,

$$H = A \cdot \sin\beta \qquad (3.7)$$

Moreover, The east-west and north-south components of the shadow, OC' (in the X-axis and Y-axis) can be calculated from these proposed modified equations,

$$P_{x_1} = P_x{}' = \frac{(A \cdot \sin\beta + H') \cdot \sin\gamma}{tan\alpha} \tag{3.8}$$

$$P_{y_1} = P_{y'} = \left(\frac{(A \cdot \sin\beta + H') \cdot \cos\gamma}{tan\alpha}\right) + A \cdot \cos\beta \tag{3.9}$$

3.3 Methodology

The design and analysis of an agrivoltaic system involve several interlinked steps, as illustrated in the methodology flow diagram in Fig. 3.3. The overall process begins with site selection, a crucial step that determines the climatic, topographical, and solar irradiance conditions necessary for accurate system modeling.

Rice (*Oryza sativa*) was selected as the representative crop in this agrivoltaic study because of its dominant role in food security and land use in Bangladesh and much of South and Southeast Asia. As the primary staple food, rice occupies a large share of cultivated land across major production systems (Aman, Boro, and Aus), making it a critical crop for assessing the practical implications of agrivoltaic deployment on regional agriculture and policy planning.

From an agrivoltaic perspective, crop responses to panel-induced shading vary with photosynthetic pathway and light demand. Maize, a C_4 crop, is generally more sensitive to reduced solar radiation and often exhibits pronounced yield losses under partial shading unless layouts are carefully optimized. In contrast, rice, a C_3 cereal, shows greater tolerance to moderate shading, with reported yield reductions typically remaining within acceptable limits, while also benefiting from modified microclimatic conditions such as reduced evapotranspiration. Although leafy greens and tuber crops may also perform well under shaded environments, their limited cultivated area, shorter growth cycles, and lower relevance to national food security make them less suitable for evaluating large-scale land-use impacts. Therefore, rice provides a more appropriate and policy-relevant basis for examining food–energy synergies in agrivoltaic systems.

Following site identification, the process bifurcates into two primary analytical paths: shadow length calculions and irradiance-based energy calculations.

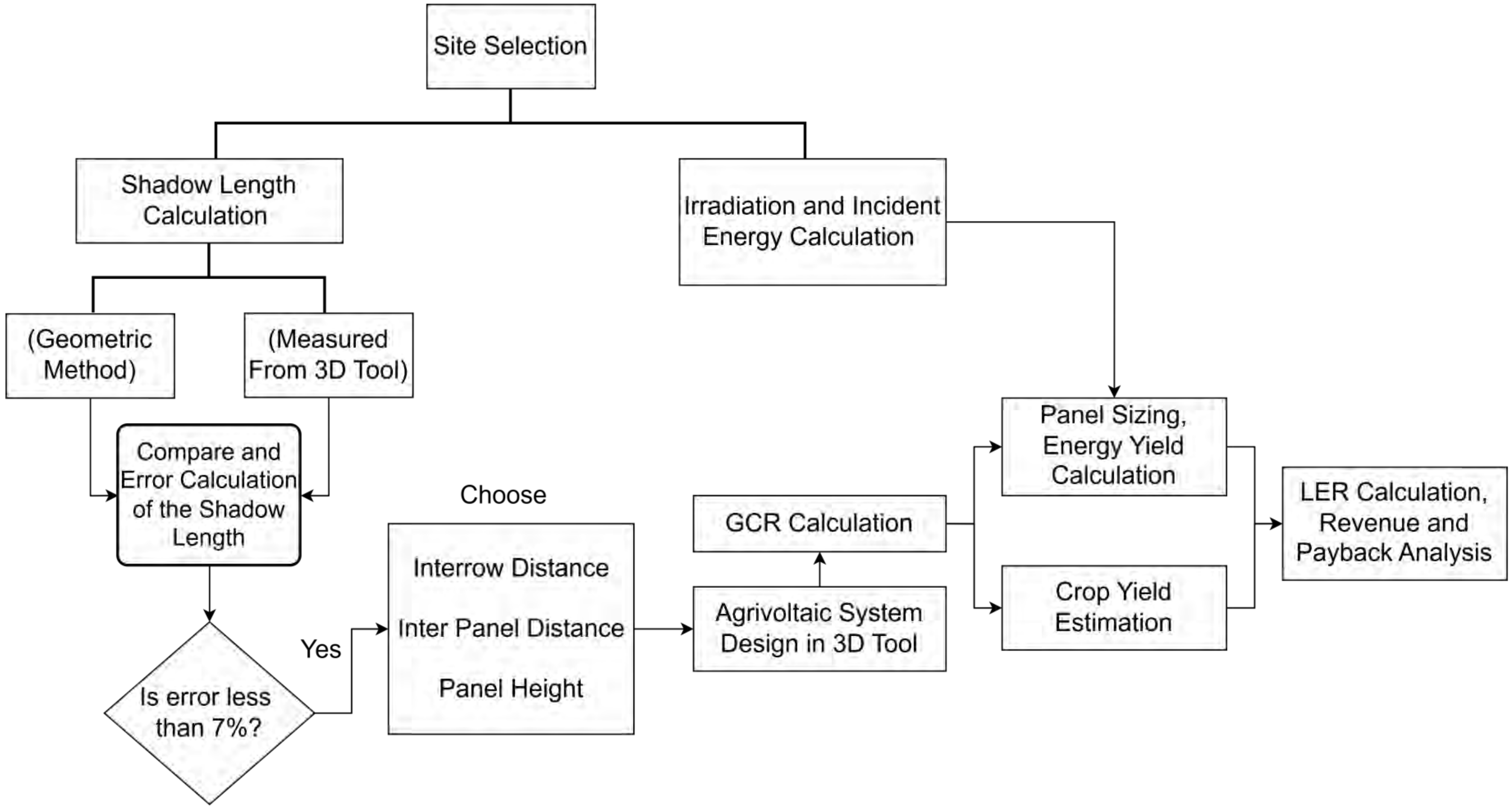

Fig 3.3. Flowchart of the methodology of the study

Geometric Shading Evaluation focuses on understanding the spatial layout of the photovoltaic (PV) system in relation to sunlight obstruction. The shadow analysis is also performed using 3D tool. After that, the two methods are compared to get the possible error. If the error is below 7% then the next stage is to set the three parameters—interpanel spacing, interrow distance, and panel height. Fig. 3.4 shows the comparative assessment flow chart of this study. These inputs help model how shadows are cast throughout the day and year. The output of this analysis is used to perform a shading impact study, which ensures that the sunlight availability for crops and panels is optimized. After designing the system for different parameters, the ground coverage ratio (GCR) is calculated.

Parallel to the shading analysis, irradiance data is calculated and used to conduct a solar panel size analysis. Based on solar resource availability, panel sizing determines the system's energy output potential. From this, the energy yield will be determined. Seperately, the crops yield will also be measured, and Land Equivalent Ratio (LER) are derived. These parameters feed into an economic feasibility assessment, specifically through a payback period estimation, to understand the system's financial viability over time.

Finally, the results from both the shading and economic assessments converge to inform a comprehensive system design that is optimized both technically and economically for agrivoltaic deployment in the selected site.

To perform the shading analysis, a particular land area (1 Hectre) has been considered. The land area is in Mymensingh district, Dhaka. The location of the land is 24.955111N, 89.533444E. The PV module considered in this study has a 170 cm width and 100 cm length. Table 3.1 shows the PV module details considered in this study.

In this study, Aman and Boro rice were selected as the representative crops for agrivoltaic assessment due to their agronomic importance and complementary seasonal coverage in

Table 3.3.: PV Panel Parameter considered in this study

Panel Length =	1.7	meter
Panel Width =	1	meter
Panel Efficiency =	15% - 23%	
Panel Avg Efficiency =	19%	0.19
Solar Irradiance =	5	KWh/ m^2/ day
Panel Output =	330	Watt

Bangladesh. Rice is the country's primary staple crop and occupies the largest share of cultivated land, playing a critical role in national food security and rural livelihoods. Aman rice is typically cultivated during the monsoon season, while Boro rice is grown in the dry winter season under irrigation. Together, these two cropping cycles span almost the entire calendar year, allowing the agrivoltaic system to be evaluated under a wide range of solar angles, climatic conditions, and crop growth stages.

In addition to their seasonal relevance, rice crops are generally considered light-demanding and less tolerant to shading compared to many horticultural or shade-adaptive crops. This characteristic makes Aman and Boro rice a conservative and challenging choice for agrivoltaic system evaluation. By focusing on crops with relatively low shade tolerance, the study aims to assess whether carefully optimized agrivoltaic designs can accommodate major staple crops without causing unacceptable yield losses. Consequently, the selection of Aman and Boro rice provides a rigorous test case for balancing photovoltaic energy generation with agricultural productivity under Bangladesh-specific conditions.

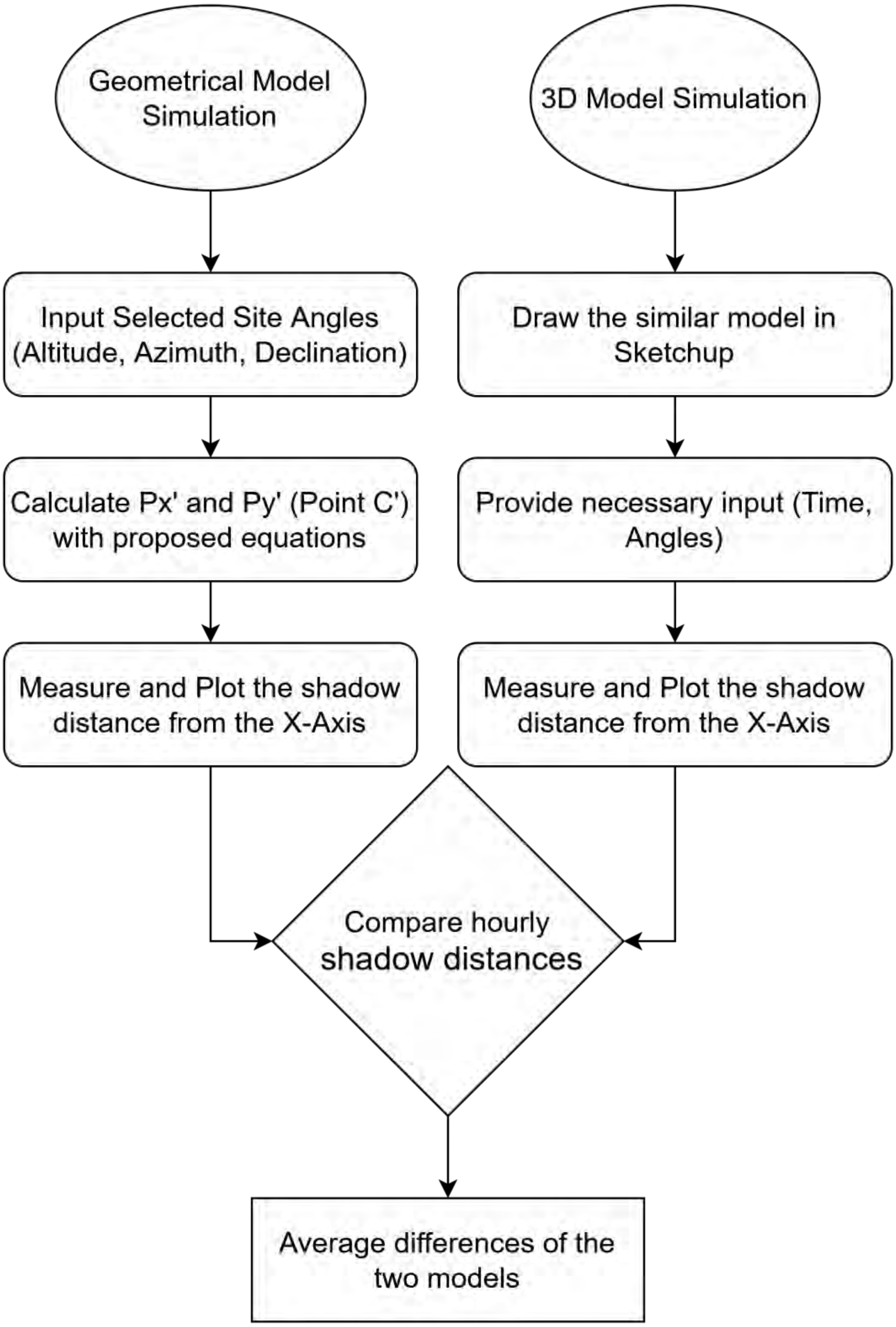

Fig. 3.4. Workflow diagram of Shadow length comparison with geometric and 3D values

Table 3.4: Design Specifications considered in this study

Design Consideration	Panel Height (cm)	Inter-Row Gap (cm)	Inter Panel Gap
Design 1	100	100	No Panel Gap
Design 2			Half Panel Gap
Design 3			Full Panel Gap
Design 4		150	No Panel Gap
Design 5			Half Panel Gap
Design 6			Full Panel Gap
Design 7		200	No Panel Gap
Design 8			Half Panel Gap
Design 9			Full Panel Gap
Design 10	500	100	No Panel Gap
Design 11			Half Panel Gap
Design 12			Full Panel Gap
Design 13		300	No Panel Gap
Design 14			Half Panel Gap
Design 15			Full Panel Gap
Design 16		500	No Panel Gap
Design 17			Half Panel Gap
Design 18			Full Panel Gap

In this study, eighteen agrivoltaic system configurations were evaluated by systematically varying key geometric design parameters. The design specifications considered include panel mounting heights of 100 cm and 500 cm, combined with inter-row gaps of 100 cm, to 500 cm. For each height–row spacing combination, three inter-panel arrangements were analyzed: no panel gap, half-panel gap, and full-panel gap.

Chapter 4

Result Analysis

4.1 Irradiation Calculation

The daily solar irradiation has been calculated with the help of irradiation model equations. Fig 4.1 shows the daily irradiation and cumulative incident energy calculated for the day 15th December considering a flat surface. The tilt angle considers zero in this case. The maximum irradiance is calculated at 720 W/m^2 for that specific day. The incident energy shows the value of 4.56 KWh/m^2.

From Fig 4.2, the average daily incident energy bar chart is shown for the flat surface or tilt angle zero-degree surface. It shows the summer months received more incident energy.

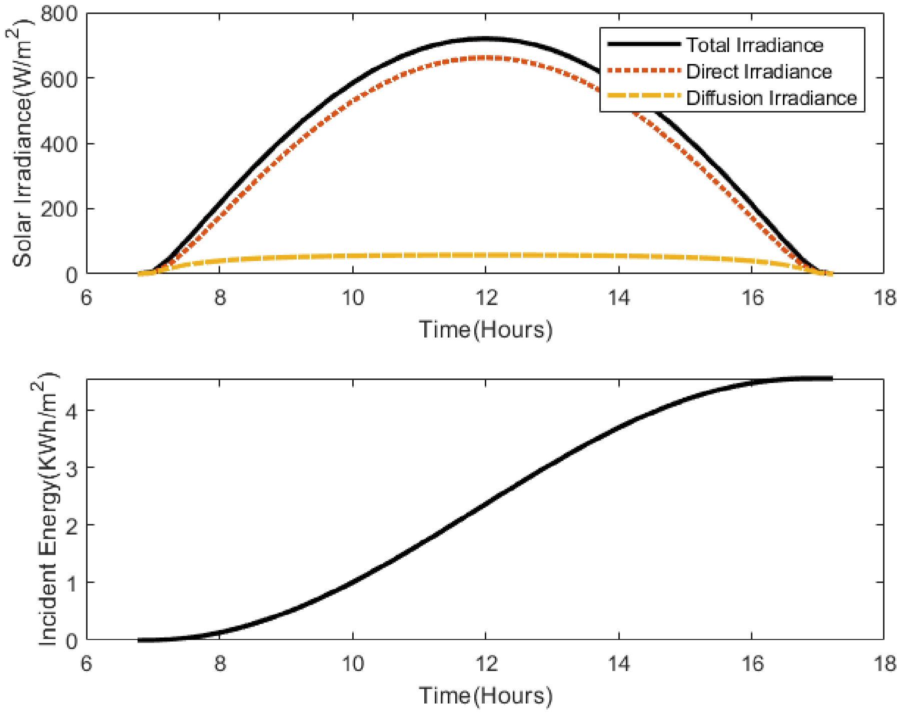

Fig. 4.1. Daily Solar Irradiance (top) and Cumulative incident energy plot (bottom) calculated for 15th December considering tilt angle zero degree.

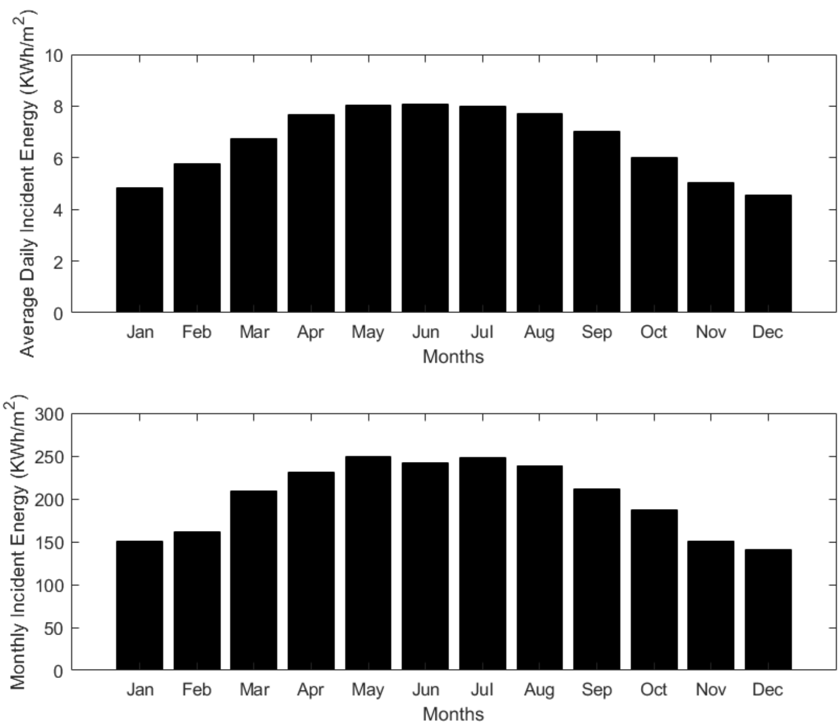

Fig. 4.2. Average Daily incident energy (top) and monthly incident energy plot (bottom) considering tilt angle zero degree.

Similarly, the monthly variation is also depicted in Fig 4.2 at the bottom bar chart. Yearly total incident energy which is accumulated is 2.42 MWh/m^2.

Fig 4.3 shows the daily irradiation and cumulative incident energy calculated for the day 15^{th} December considering a tilt surface. The tilt angle considers 24.955 as the lattitude angle of the site in this case. The maximum irradiance calculated 969 W/m^2 for that specific day. The incident energy shows the value 6.48 KWh/m^2, which is significanly higher than the flat surface.

From the Fig 4.4, the average daily incident energy bar chart is shown for the tilt angle 24.955 degree surface. Yearly total incident energy which is accumulated is 2.66 MWh/m^2, which is significantly higher (almost 10%) than the flat surface.

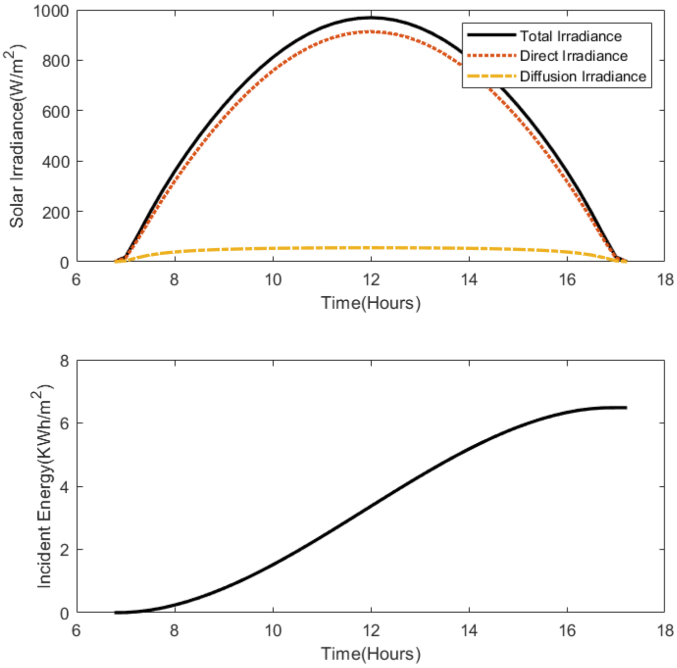

Fig. 4.3. Daily Solar Irradiance (top) and Cumulative incident energy plot (bottom) calculated for 15th December considering tilt angle 24.955 degree.

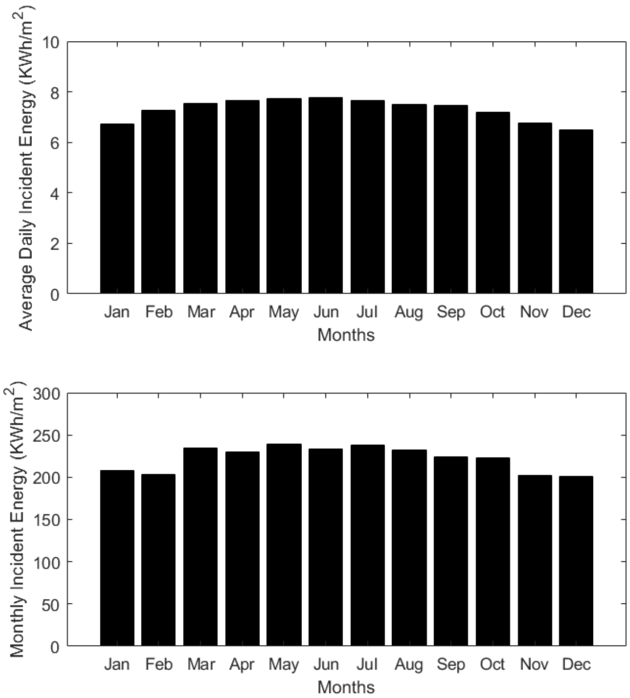

Fig. 4.4. Average Daily incident energy (top) and monthly incident energy plot (bottom) considering tilt angle 24.955 degree.

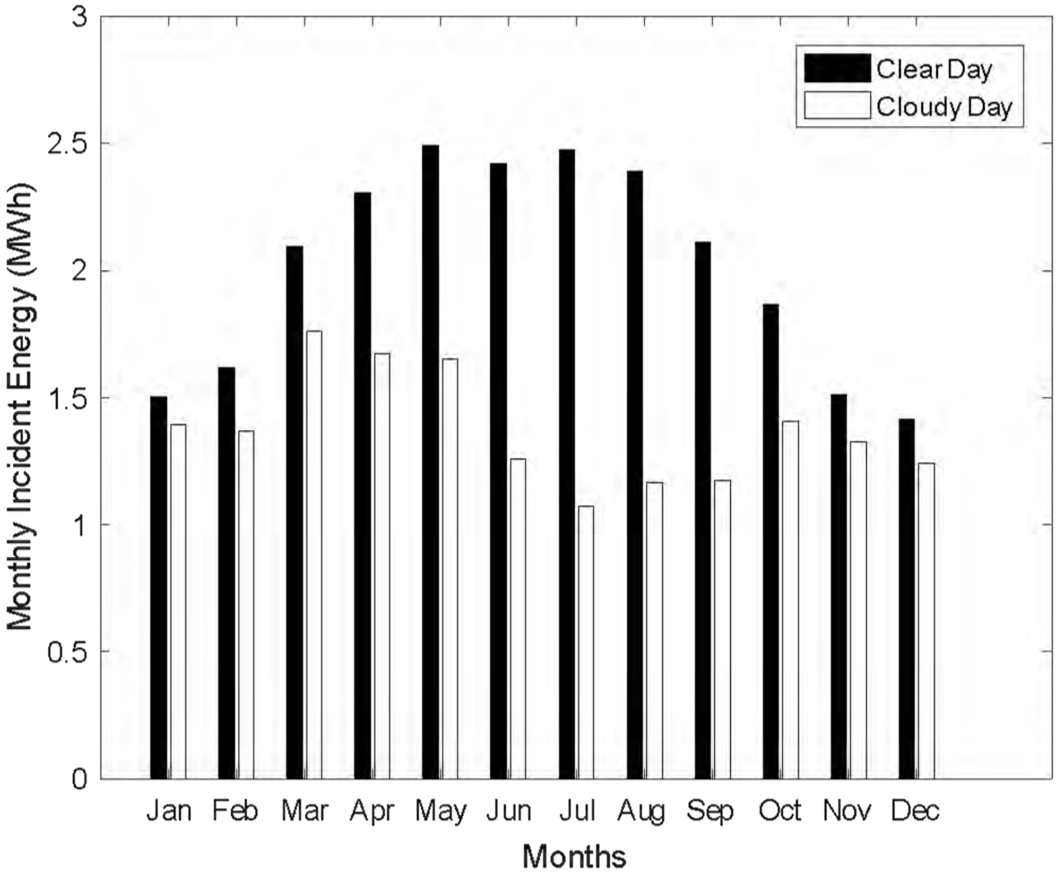

Fig. 4.5. Monthly Average Incident Energy Plot for 1 Ha. Land area (fixed flat surface) considering clear and cloudy days.

For the selected site area of 1 hectre, the calculated total annual energy for clear and cloud day is 24.2065 MWh and 16.4845 MWh respectively. The cloudy day reduces the significant amount of incident energy on the flat surface over the year. Figure 4.5 shows the bar chart of the monthly average incident energy plot for 1 Ha. Land area (fixed flat surface) considering clear and cloudy days. Whereas for the tilt surface, total annual energy of 1 Hectre area for clear and cloud day is 26.6883 MWh and 18.6795 MWh respectively. Which is 11% more than the flat surface considering cloudy days. So, for agrivoltaic system, this study considers only the fixed tilted system equal to the latitude angle facing to the south. Figure 4.6 depicts the bar chart for monthly average incident energy for 1 Hectare land area (fixed tilted surface) considering clear and cloudy days.

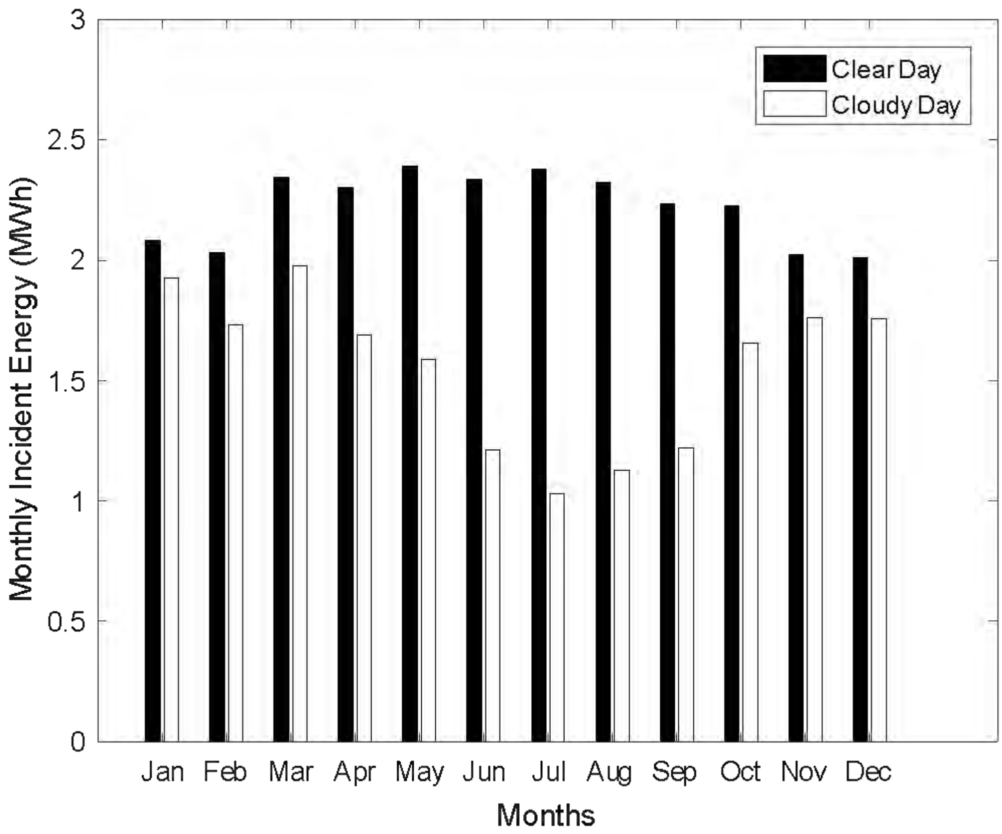

Fig. 4.6. Monthly Average Incident Energy Plot for 1 H. land area (fixed tilted surface) considering clear and cloudy days.

In this study, fixed-tilt photovoltaic (PV) modules were selected due to their structural simplicity, lower capital cost, ease of construction, and proven reliability under local conditions in Bangladesh. Alternative PV layouts—such as checkerboard or staggered row configurations, which enhance light uniformity on the ground, and vertical bifacial PV systems oriented east–west, which reduce midday shading while extending generation into morning and evening periods—were not considered in this work due to increased structural complexity, higher installation costs, and limited regional operational data. Moreover, vertical and non-continuous layouts often require more advanced modelling of bidirectional irradiance, albedo effects, and crop-specific light interception, which were beyond the scope of the present analysis.

4.2 Geometric Shading Analysis

4.2.1 Shadow Components

In this study, the shadow behavior of the inclined edge of a solar collector Panel has been analyzed for December 15, and the results are illustrated in Figure 4.7. Figures 4.7(a) and 4.7(b) depict the shadow projections along the north-south and east-west axes, respectively, as they vary over time. It is evident from the plots that around solar noon, the X-axis shadow components are nearly zero, and the Y-axis shadows are relatively short in length. During this

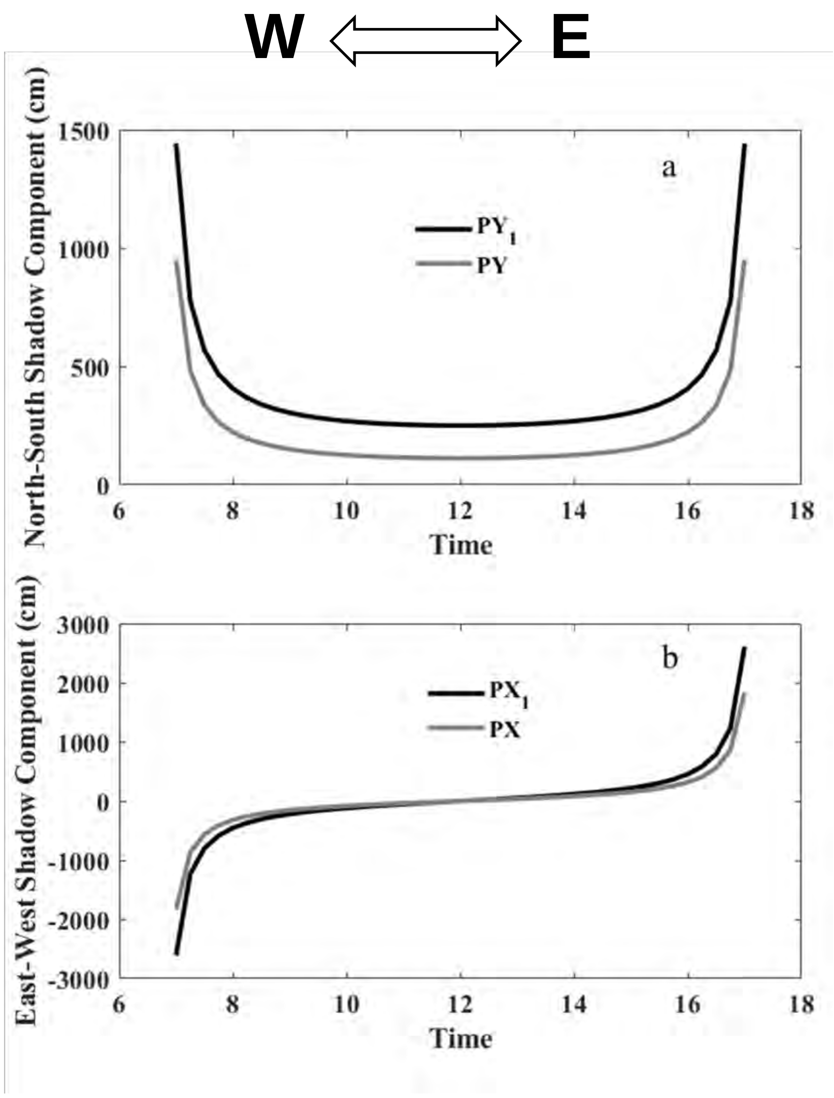

Fig. 4.7 North-South (a), East-West (b) shadow component of an inclined side edge of the solar collector on December 15th.

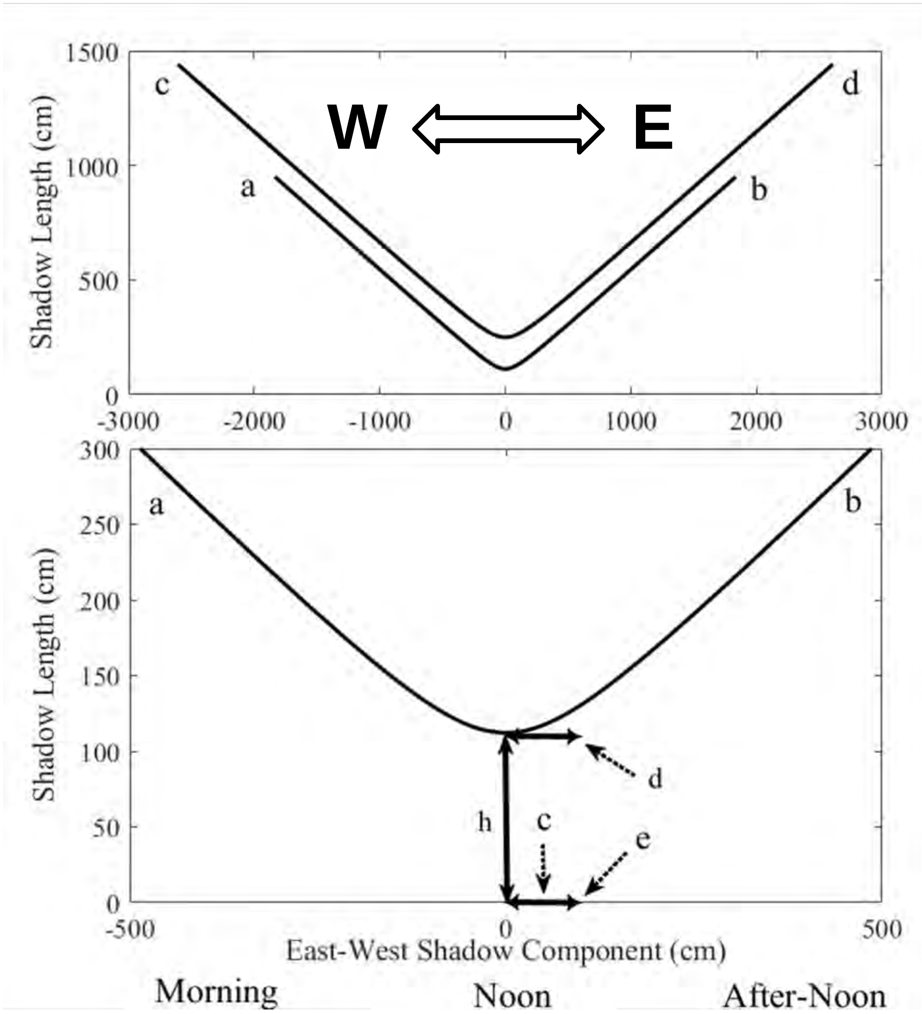

Fig 4.8 Shadow variation of an inclined collector Panel (top) and P osition of the inclined collector (bottom) on December 15th.

period, the Y-axis shadow extends northward, while significantly longer shadows are observed during early morning and late afternoon hours. For this analysis, the focus has been on the shadow cast by the inclined edge of the collector. In this study, the shadow component of the inclined collector edge has been considered, where the shadow length region consists of P_{YI} and P_{XI} has been observed to determine the inter-row, and inter-collector distance.

Figure 4.8 illustrates the variation in shadow length throughout the day, capturing both the X-axis and Y-axis components of the shadows cast by inclined solar collector Panels. In the upper portion of the figure, area labeled 'cabd' represents the shadow zone, where segments "ab" and "cd" correspond to the shadow projections from the lower and upper edges of the inclined collector, respectively. In this analysis, the shadow length denoted as "cd" has been particularly important for estimating the appropriate inter-row spacing and distance between adjacent collectors. In the lower part of the figure, "e" marks the base position of the inclined collector, "c" indicates the physical width of the collector (170 cm), "h" represents the vertical distance from the collector edge to its corresponding shadow at solar noon, and "d" identifies the endpoint of the shadow cast by the collector.

4.2.2 Monthly Shadow Length Variations

Figure 4.9 illustrates how the east-west components of shadow and the average daily shadow lengths vary across different months for an inclined solar collector positioned at the origin. From the analysis, it is evident that December exhibits the longest and widest shadow projection compared to other months. At solar noon, the upper edge of the collector casts a shadow measuring approximately 250.2 cm. Given that the collector has a width of 170 cm and is installed at a certain tilt angle, the effective shaded length on the ground (denoted as 'b') is

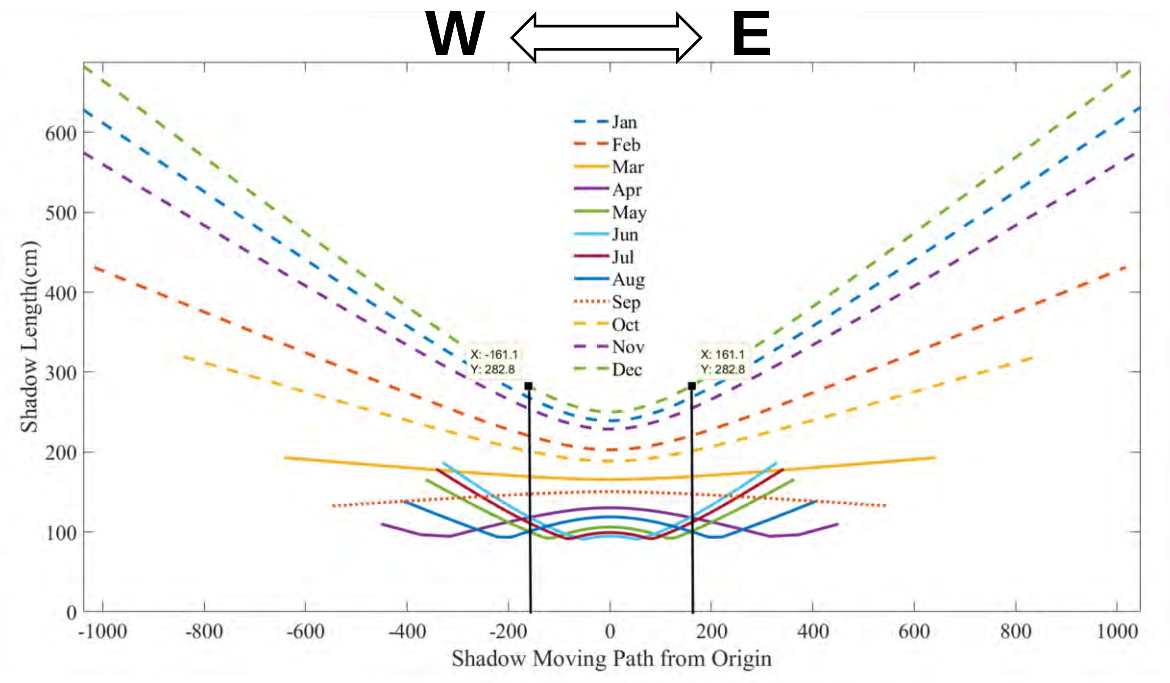

Fig. 4.9. Relationship between east-west shadow components and average daily shadow lengths for each month of the inclined collector Panel (side) at a height of 100 cm.

computed to be 90.67 cm. June has the shortest shadow distance of any other month from the X-axis. Shadow distance from the X-axis varies in "U" –shaped pattern. It is also clear that winter months (Oct-Feb) shows the wider shadow patterns (dashed lines) whereas the summer months show the shadow pattern is less wider (dark lines).

4.2.3 Height impact on Shadow Length

In agrivoltaic systems, solar panels must be elevated above ground level to ensure sufficient clearance for farming activities, including tractor operation and farmer movement. To evaluate how panel height influences shadow behavior, a comparative analysis was conducted at three different elevation levels: 100 cm, 200 cm, and 300 cm. Figure 4.10 presents the relationship between the east-west shadow components and the corresponding daily shadow lengths for three representative months—January (black lines), May (blue lines), and September (red lines)—based on the left-edge shadow of an inclined panel support Panel.

The analysis shows that in January, increasing the panel height causes the shadow to extend farther, indicating a need for wider spacing between rows to prevent shading of adjacent panels. In contrast, during May, the shift in shadow with increased height is minimal, largely due to the higher solar altitude. September, however, shows a more noticeable shift in shadow position with height changes, though not as extensive as January.

Table 4.1. Height Impact on Shadow Analysis

PV Panel Height from the Ground in cm	**Shadow length difference at origin for January**	**Shadow length difference at origin for May**	**Shadow length difference at origin for September**
100cm- 300cm	208 cm	21 cm	84 cm

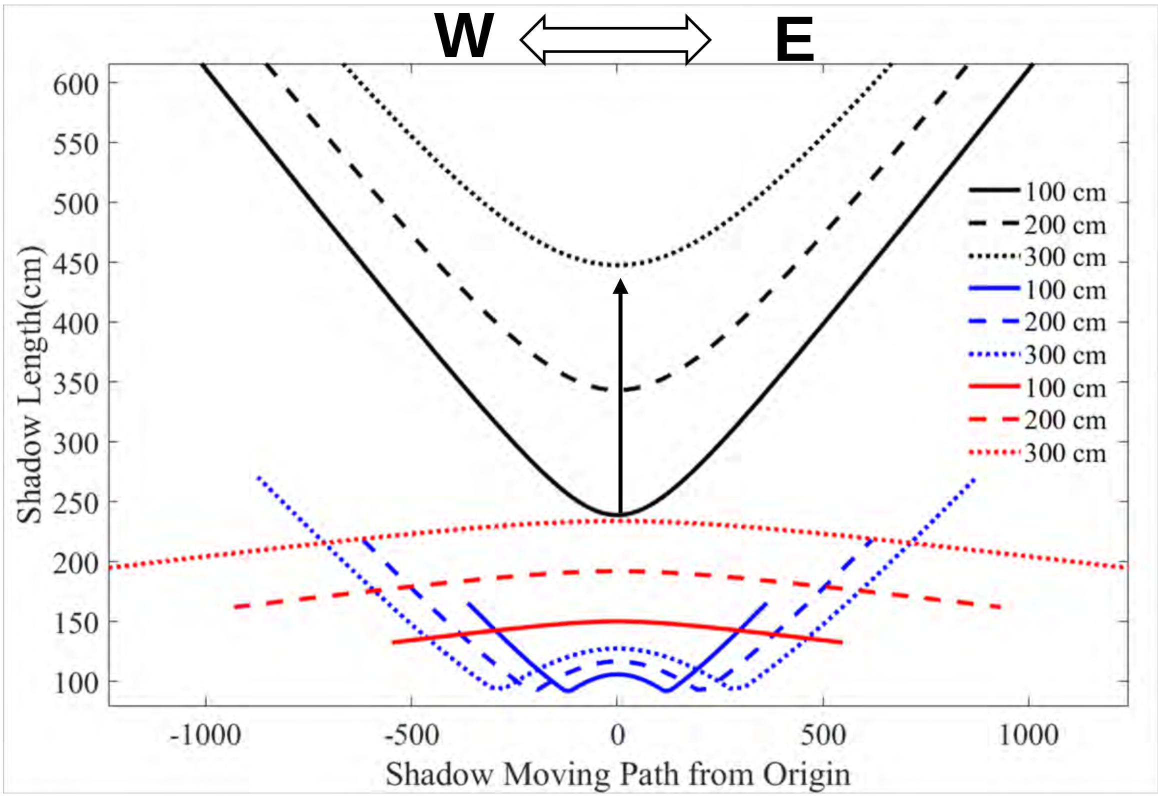

Fig. 4.10. Relationship between east-west shadow components and average daily shadow lengths for the month of January (black lines) , May (Blue lines) and September (Red lines) of the inclined collector Panel (side) at the height of 100 cm, 200 cm and 300cm.

This pattern is further clarified through simple calculations provided in Table 4.1. Specifically, in January, the shadow at the base of the Panel shifts by as much as 208 cm, the greatest displacement among the three months studied. This suggests that during winter, taller panel installations result in more pronounced shadow movement, while in summer (e.g., May), the influence of height on shadow position is relatively minor. Hence, it can be concluded that panel height has a more significant effect on shading during the winter months compared to summer.

4.3 Shadow Analysis

4.3.1 Shadow Length Analysis in 3D tool

The model with similar panel and height is designed in the 3D tool named SketchUp as shown in Fig 4.11. The shadow edge positions C (Px, Py) and C' (Px', Py') are caused by the inclined panel where OC and OC' from the origin can be obtained from the X-axis and Y-axis components.

SketchUp was used for three-dimensional geometric modeling and shadow visualization because it can incorporate site-specific geolocation data and clearly represent shading behavior in a spatial environment. The software allows users to define key parameters such as latitude,

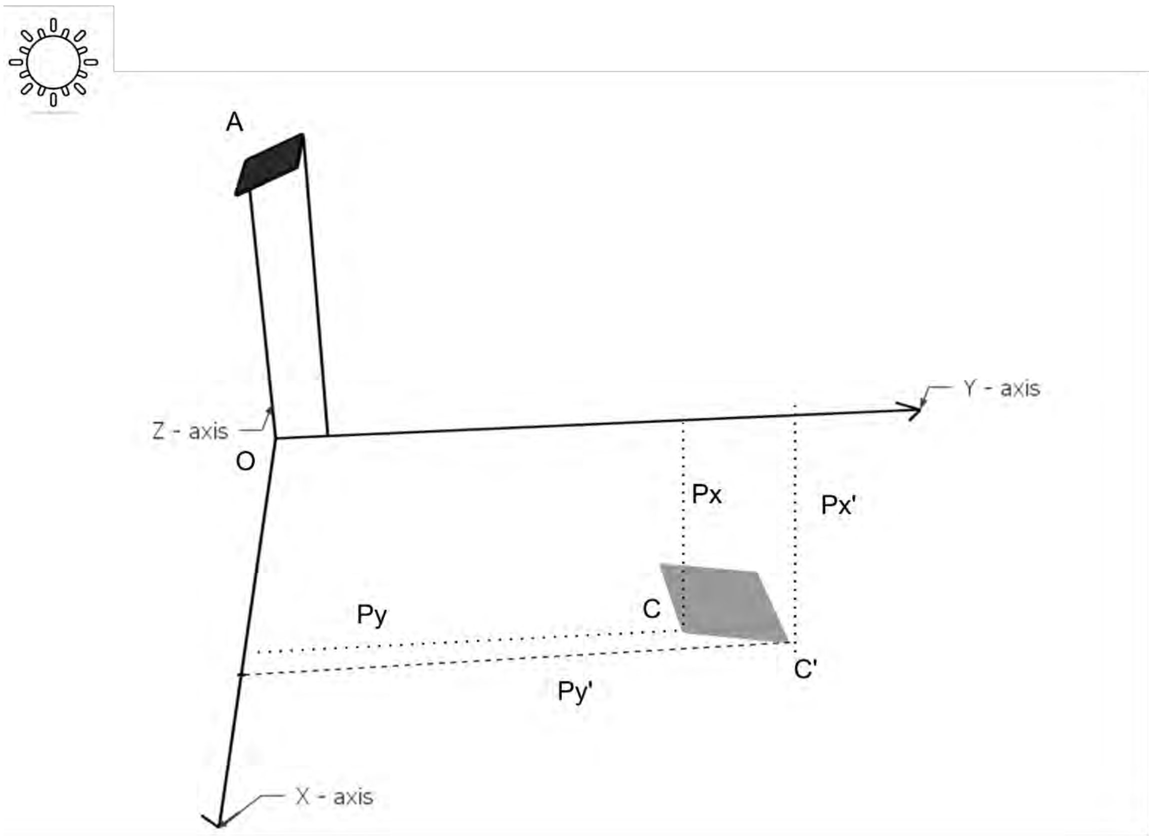

Fig. 4.11. Shadow components of an inclined Panel above the origin in a 3D model.

Table 4.2. Shadow length of the system with 100 cm Height calculated in geometric model and measured in 3D Tool at 9 a.m. and 12 p.m. for the 15th day of the each month

	Shadow Length (3D Tool) (cm)		**Shadow Length (Geometric Model) (cm)**		
	9:00 AM	**12:00 PM**	**9:00 AM**	**12:00 PM**	
15-Jan-24	285	232.6	290	248	**100 cm Panel Height**
15-Feb-24	223.9	195.7	226	206	
15-Mar-24	165.7	159.5	167	163	
15-Apr-24	118.2	126	120.3	130.2	
15-May-24	88.8	103.3	92.2	105	
15-Jun-24	87.4	93.1	106.6	94.7	
15-Jul-24	88.4	97.4	101.1	99.1	
15-Aug-24	103.8	116.1	105.2	118.7	
15-Sep-24	144.6	144.9	147.6	150.3	
15-Oct-24	193.8	181.1	203.4	188.6	
15-Nov-24	250.1	220.6	270	236	
15-Dec-24	293	243.8	341	260	

longitude, panel orientation, and simulation date and time, which are essential for analyzing agrivoltaic systems.

Although the internal shadow calculation algorithm of SketchUp is not publicly documented, the platform has been widely applied in previous solar energy and shading studies as a reliable visualization tool. Many studies have demonstrated that, when SketchUp results are crosschecked with established solar position models or field measurements, the predicted shadow patterns show good agreement.

In this study, SketchUp was therefore employed to visually demonstrate seasonal shadow variations and the spatial interaction between photovoltaic panels and agricultural plots. It also served as an independent reference to validate the accuracy of the proposed geometric shadow calculation method. Table 4.2 shows the calculated shadow length for 100 cm height of PV panel for the 14th of November at 9 a.m. and 12 p.m.

4.3.2 Shadow Length Error Analysis-Geometric and 3D Model

Figure 4.12 presents bar charts comparing shadow lengths obtained from geometrical calculations in MATLAB and 3D simulations in SketchUp for the 15th day of November considering panel height of 100 cm (top) and 500 cm (bottom). For 15 November 2024, both models show the longest shadows at 9 AM and 3 PM. The shortest shadow lengths occur near midday. The geometrical calculation shows slightly higher values than the 3D model.

However, the error calculation shows that the shadow length of C’ point of the two methods; geometrical and the 3D model does not exceed 7% throughout the year. Which depicts that the geometric model could be used for designing agriPV system for shading analysis with a yearly error of less than 7%. Fig. 4.13 shows the percentage error in shadow length calculated in geometric model and 3D tool for 100 cm panel height simulated in each 15 days of all months. The shadow distance error depicted in this figure is calculated for 12 p.m. each day. Bar chart shows that May has the lowest shadow difference and November has the highest one.

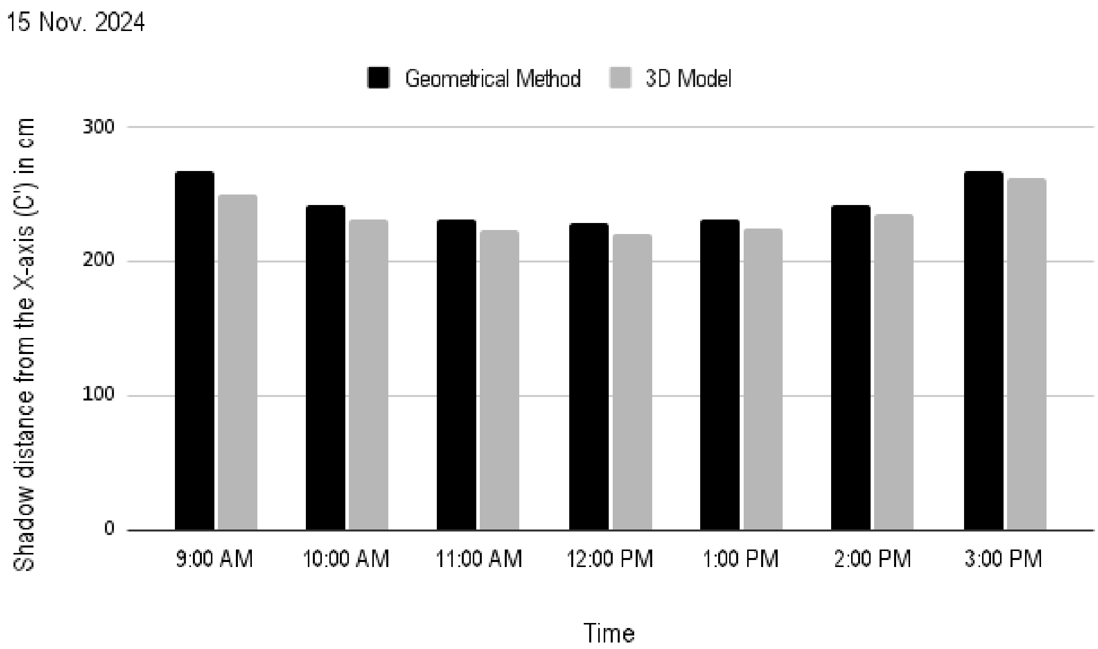

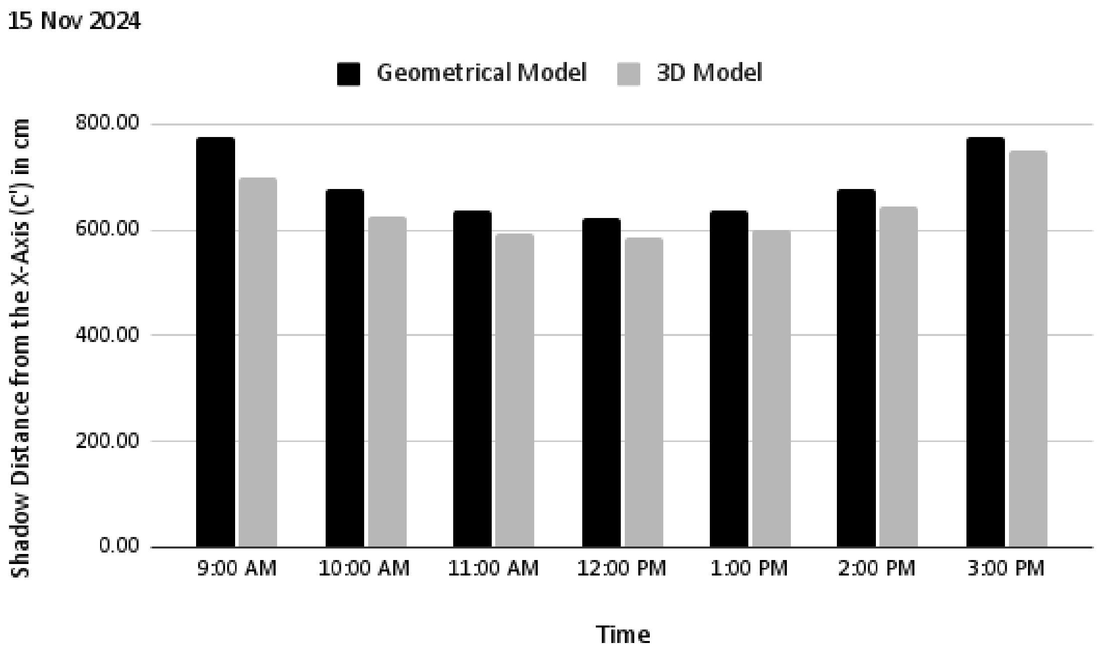

Fig. 4.12. Comparative bar chart of shadow distance variation calculated geometrically and 3D modelling for the 15 November considering panel height of 100 cm (top) and 500 cm (bottom).

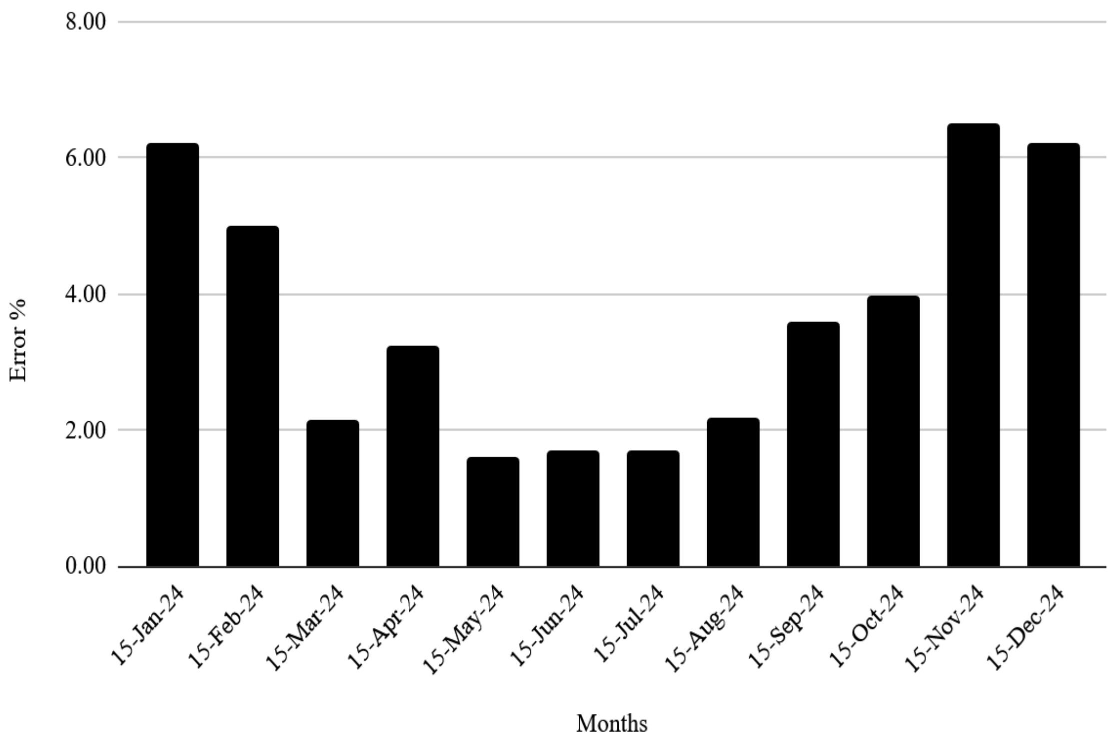

Fig. 4.13. Percentage of error in shadow length calculated in geometric model and measured in 3D tool for different months of the year 2024 at 12 PM.

A modelling error of approximately 10% is considered acceptable in agrivoltaic shadow and irradiance analysis due to the complexity of processes, including dynamic solar geometry, partial shading, and spatial variability in light distribution. Complete elimination of modelling error is therefore impractical, and validation is commonly assessed against established tolerance thresholds. Recent literature indicates that relative errors below 10% are widely regarded as suitable for agrivoltaic performance evaluation and comparative design analysis. Zainali et al. (2025) reports that validated agrivoltaic simulation studies frequently achieve irradiance-related errors within this range and consider such accuracy sufficient for system design, optimisation, and decision-making [71]. Consequently, the observed below 10% deviation between the geometrical model and SketchUp-based simulation falls within accepted limits and does not significantly affect the robustness of design conclusions.

4.4 System Design for Analysis

To evaluate the influence of structural geometry on shading behavior, energy yield, and crop exposure, a systematic set of agrivoltaic layout configurations was defined by varying panel height, inter-row spacing, and inter-panel gap. Two representative mounting heights were selected, namely 100 cm and 500 cm, to capture the effects of low-mounted and elevated PV structures on seasonal shadow distribution. For each height, three inter-panel gap conditions were considered: no panel gap, half panel gap, and full panel gap, representing increasing levels of horizontal spacing between adjacent modules within a row. In this study, a half panel gap is

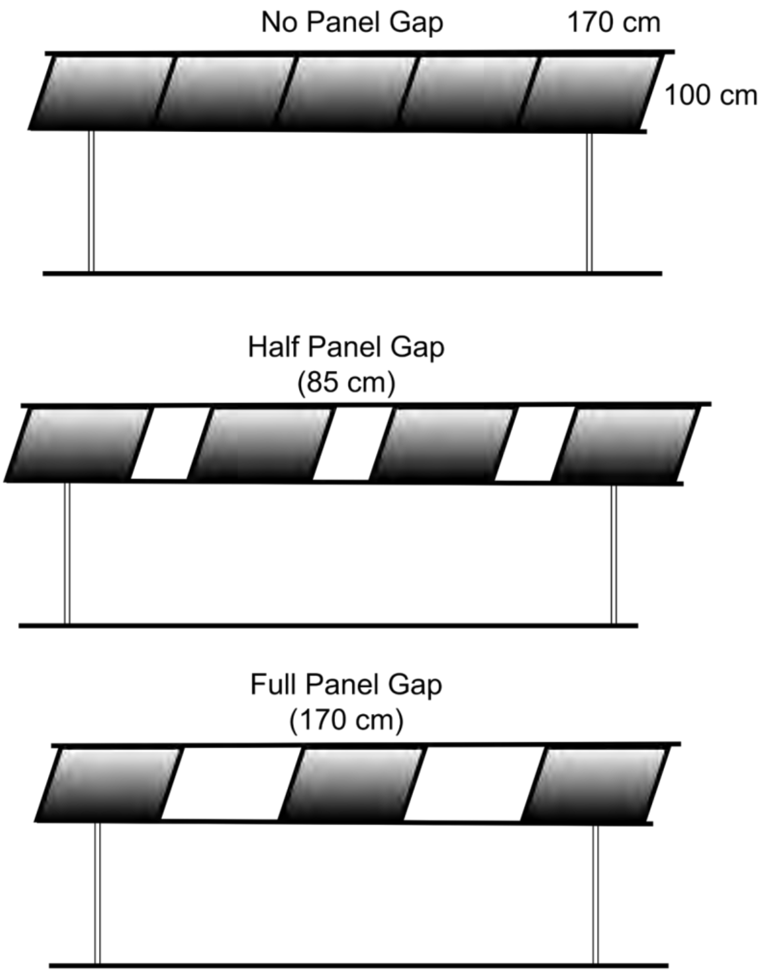

Fig. 4.14. Visualization of inter-panel distance of no panel gap, half-panel gap (85 cm) and full panel gap (170 cm).

defined as an inter-panel spacing corresponding to 50% of the width of the selected photovoltaic module. Figure 4.14 shows the inter-panel separation considered in this study.

At the lower mounting height of 100 cm, inter-row spacing values of 100 cm, 150 cm, and 200 cm were examined under each inter-panel gap condition, resulting in nine distinct layout scenarios. This range was chosen based on the shadow length calculations to reflect compact agrivoltaic installations where land-use intensity is high and shading interactions are more pronounced. In contrast, for the elevated mounting height of 500 cm, wider inter-row spacing of 100 cm, 300 cm, and 500 cm was analyzed, again across all three inter-panel gap configurations. Figure 4.15 visualizes the inter-row distances which are considered to design the system.

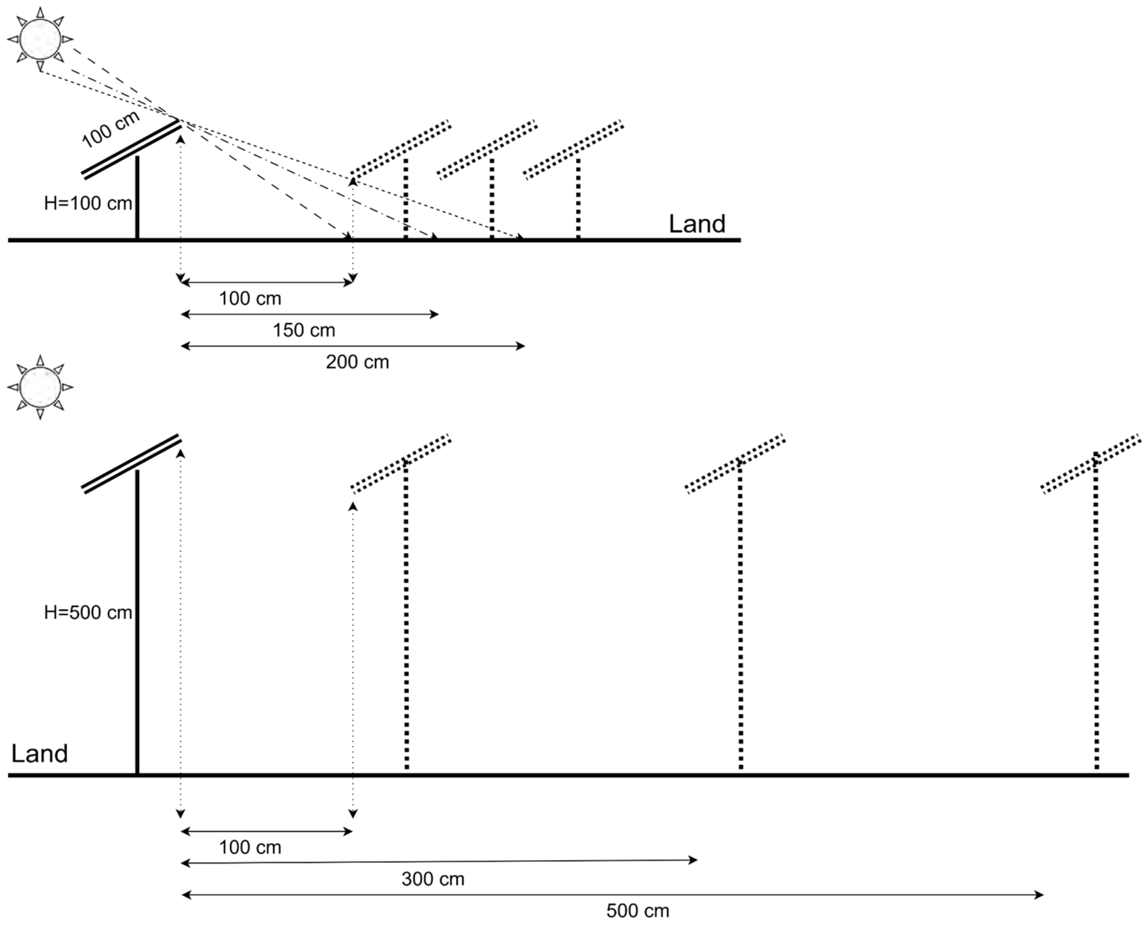

Fig. 4.15. Visualization of inter-row distances for 100 cm and 500 cm panel height.

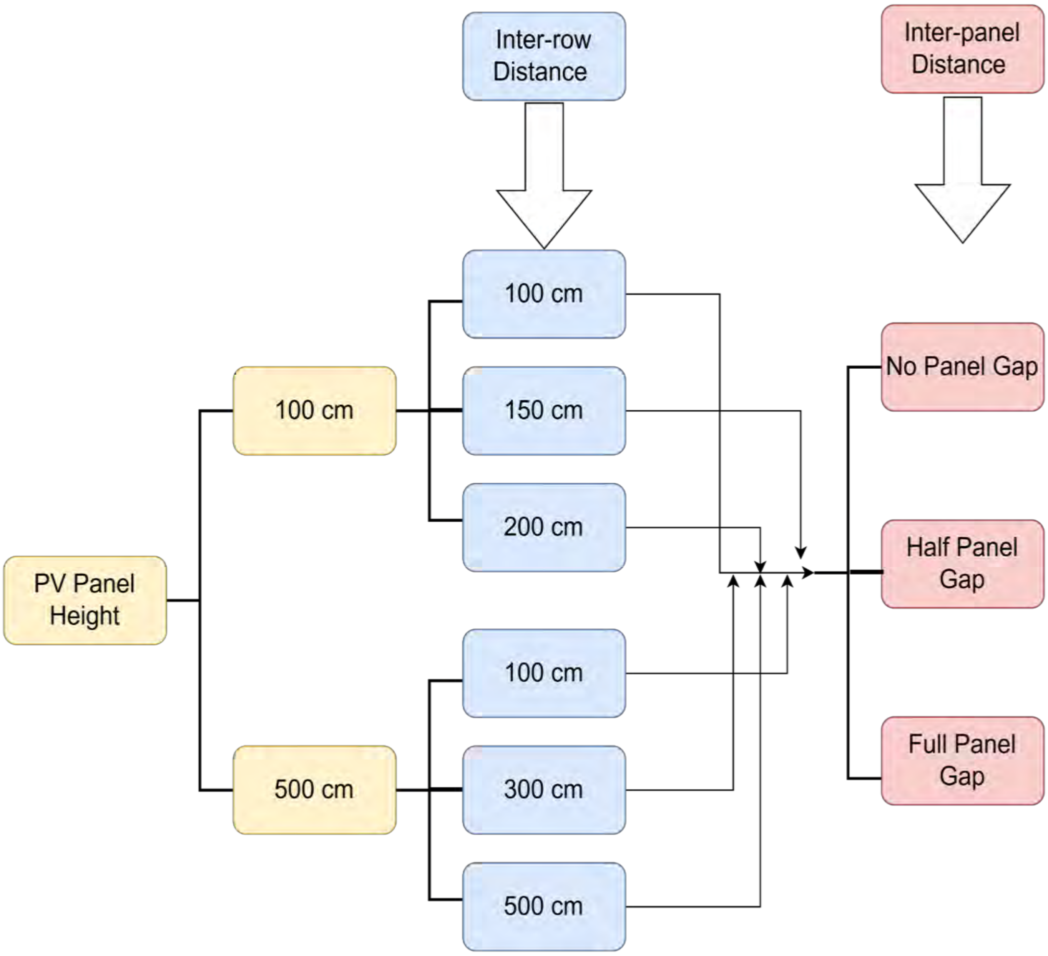

Fig. 4.16 Chart of Considered System parameters (i.e. inter-row gap, inter-panel gap, and height of the PV panel) for design and analysis.

These layouts represent more open agrivoltaic systems intended to reduce crop shading and improve agricultural accessibility. It is found from the simulation that selected parameters do not create shadow overlapping in the system. Figure 4.16 shows the chart of considered design parameters.

Now for the design implication, 3D design has been considered to observe the shading variation and visualize the actual shading pattern for two specific seasons which are summer season and winter season because of two different types of selected rice crops. These are Aman Rice which

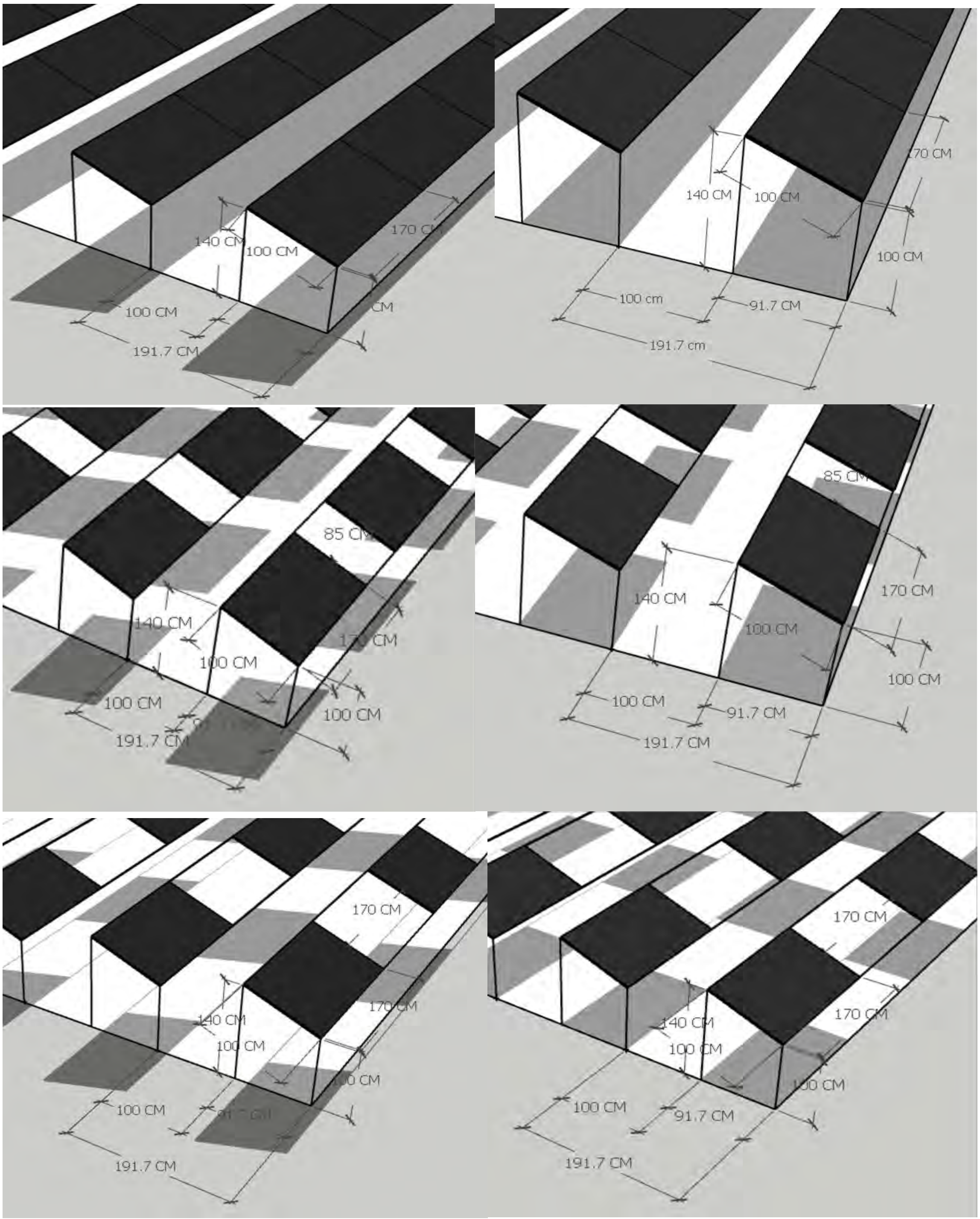

9 a.m. 12 p.m.

Fig. 4.17. Daily shadow simulation at 9 a.m. and 12 p.m. for 100 cm Height, 100 cm Inter-row Gap, and No Inter Panel Gap (top), Half Inter Panel Gap (middle) and Full Inter Panel Gap (bottom) Simulated on 15 June 2024.

is suitable for summer season and other one is Boro Rice which is suitable for winter season. Moreover, the daily shading variation has also been assessed by taking two different day time in a whole day which are 9 AM (morning time) and 12 PM (solar noon time).

In Fig. 4.17, analyzed shading patterns for 100 cm elevated panel configurations with 100 cm inter-row gap between each row with three different panel distributions such as “No Panel Gap”, “Half Panel Gap” and lastly “Full Panel Gap”. All these 3D simulated designs are for 9 AM morning time (left) and 12 PM solar noon time (right). The motivation behind selecting two different daytimes, such as 9 AM and 12 PM, is to visualize shading impact on the landscape during the whole day and how shading pattern on the crop level changes with time as well yearly. Moreover, with the season variations, it is noticed how shadow length changes with various seasons for a whole year. Normally in the month of June 2024, Bangladesh observes summer season meaning that in that month agrivoltaic systems will observe shorter shadow length because of higher declination angle of the sun on the crop level with longer daytime. As the summer months represent shorter shadow lengths, the shading impact on the ground level is very close to the inclined edge.

Fig. 4.18 shows the daily shadow simulation at 9 a.m. and 12 p.m. for 500 cm Height, 500 cm Inter-row Gap, and No Inter Panel Gap (top), Half Inter Panel Gap (middle) and Full Inter Panel Gap (bottom) Simulated on 15 December 2024. This month represents winter season in Bangladesh, and because of that the agrivoltaic systems observe longer shadow length due to decrease in declination angle of the sun as well as shorter daytime. Due to decrease in declination angle of the sun, the crops underneath the panels observe longer shadow length in the ground level with shorter daytime.

From the designs, the number of rows, panels and aeas can be calculated to use for further calculations i.e. ground coverage ratio, land equivalent ratio etc.

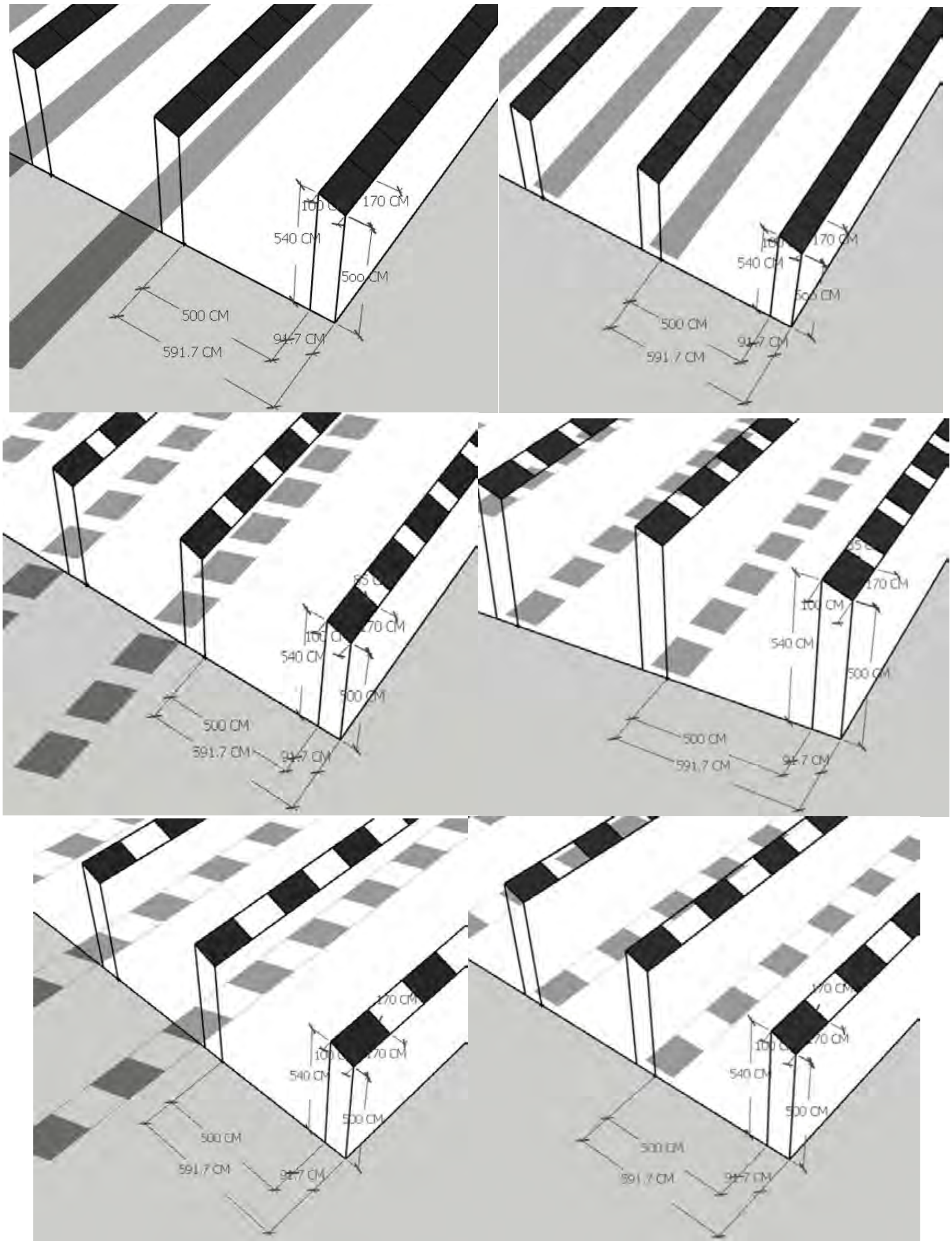

9 a.m. 12 p.m.

Fig. 4.18. Daily shadow simulation at 9 a.m. and 12 p.m. for 500 cm Height, 500 cm Inter-row Gap, and No Inter Panel Gap (top), Half Inter Panel Gap (middle) and Full Inter Panel Gap (bottom) Simulated on 15 December 2024.

4.4.1 GCR vs No. of PV Panel

Based on the design simulated in the SketchUp, ground coverage ratio (GCR) has been calculated. As the inter-row and inter-panel distance is selected, the number of rows and number of total PV panels can be calculated. The calculation of the panel is directly related to the inter-row distance. Fig. 4.19 shows the relation of the inter-row distance with the number of panel rows. It depicts that the inter-row distance which varies from 100 cm to 500 cm reduces the overall number of rows 67%.

From Fig. 4.20, it shows the relation between the Ground Coverage ratio vs calculated number of PV Panels for the selected 1 Hectare land. The relationship is linear and the increase in GCR of 0.1, number of panels increases 47%. It means that the more the GCR, the greater number of PV panels.

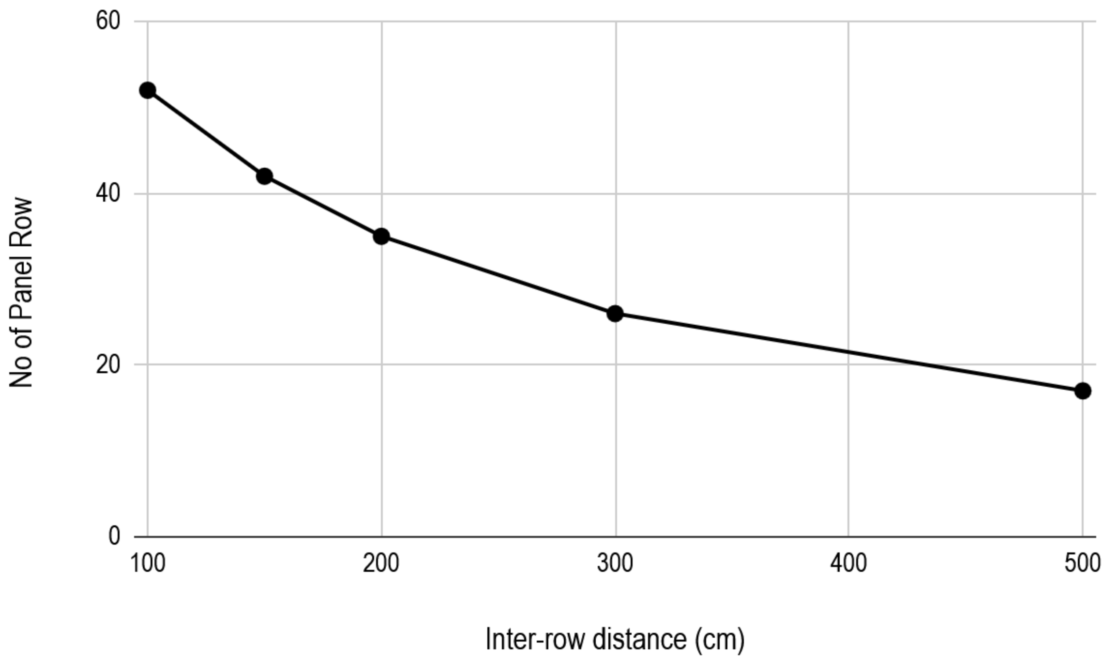

Fig. 4.19. Relation of the inter-row distance with the number of panel rows.

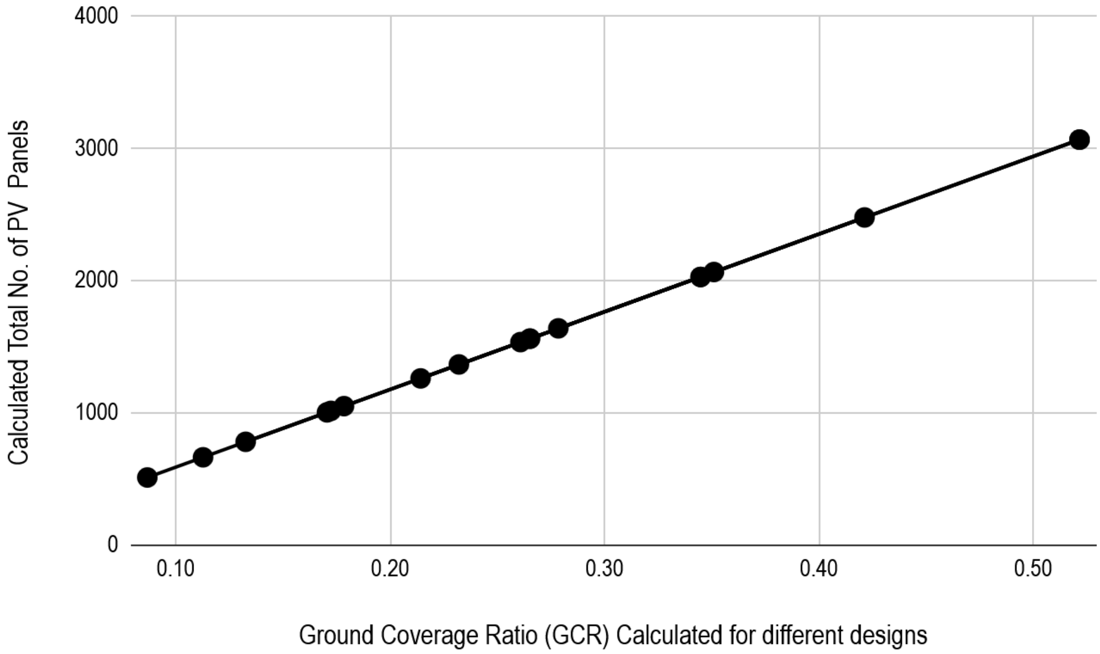

Fig. 4.20. GCR vs Number of PV Panels for the systems considered in this study.

4.4.2 GCR vs Relative Yield of Crops

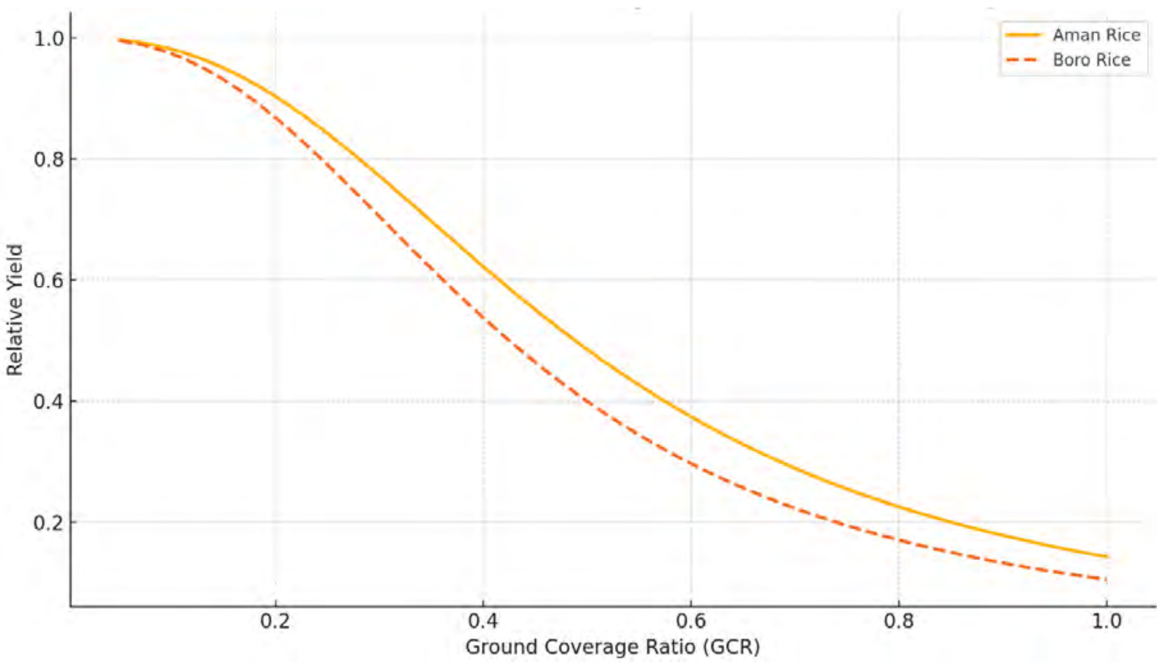

Fig. 4.21. Ground Coverage Ratio (GCR) vs Relative Crop Yield of Aman and Boro Rice.

To calculate the relative yield for crops, a straightforward approach has been taken. For that, based on several research papers [60-70] Ground Coverage Ratio (GCR) and Relative Crop Yield have been plotted for both Aman and Boro Rice in Fig. 4.21. Calculating the Ground Coverage ratio from the system design, the relative crop yield could be found from the plot for further calculations of Land Equivalent Ratio. Figure shows that the relative Crop Yield is decreasing when the GCR values increase. That means the more shaded area in the field, the crops production will be degraded.

Yield value has been taken for the Mymensingh region. Boro crops have a higher yield than Aman, However, the Boro crops are less shade tolerant than Aman. Here, specific variant did not consider, rather value is taken to assess the systems in a generalized way. The yield value of the Aman crops is considered 4983 kg/Ha and for Boro it is taken as 6332 kg/Ha [59].

4.4.3 LER vs GCR

After calculating the relative yield of the crops with respect to GCR, relative yield of the energy will be calculated. As number of panels and panel area is known, from that daily energy is calculated and compared to the energy calculated only for the PV system exists. From the crops and energy yield, Land Equivalent Ratio can be calculated. Result show that, if the inter-row gap varies for a specific height and specific inter-panel gap, the GCR and the relative yield for energy linearly decrease. Whereas the crop yield linearly increases. For two crops in one-year system, overall impact is negligible in LER. Figure 4.22 (a) shows that the Land Equivalent Ratio (LER) spans from 1.14 to 1.27 across all configurations where GCR varies 0.10~0.50. Here most of the design options achieve LER values between 1.20 and 1.27, which can be considered the optimal range. The variation is negligible whether the GCR value is increasing. It represents consistently high land-use efficiency for most of the agrivoltaic layouts analyzed in this study.

Fig. 4.22(b) shows GCR, relative yield (RY) for energy, relative yield (RY) for crops and Land Equivalent Ratio (LER) calculated for different agrivoltaic design parameters considering 100 cm panel height (top) and 500 cm panel height (bottom).

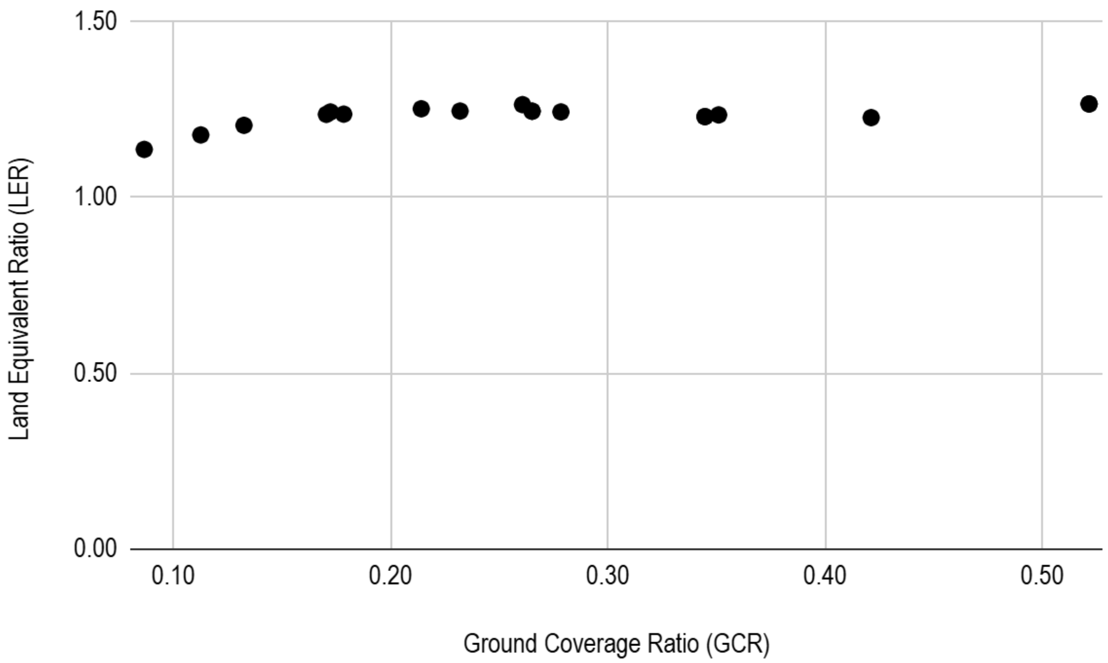

Fig. 4.22 (a). Land Equivalent Ratio (LER) vs Ground Coverage Ratio (GCR) calculated for different agrivoltaic design parameters considering 100 cm and 500cm panel height.

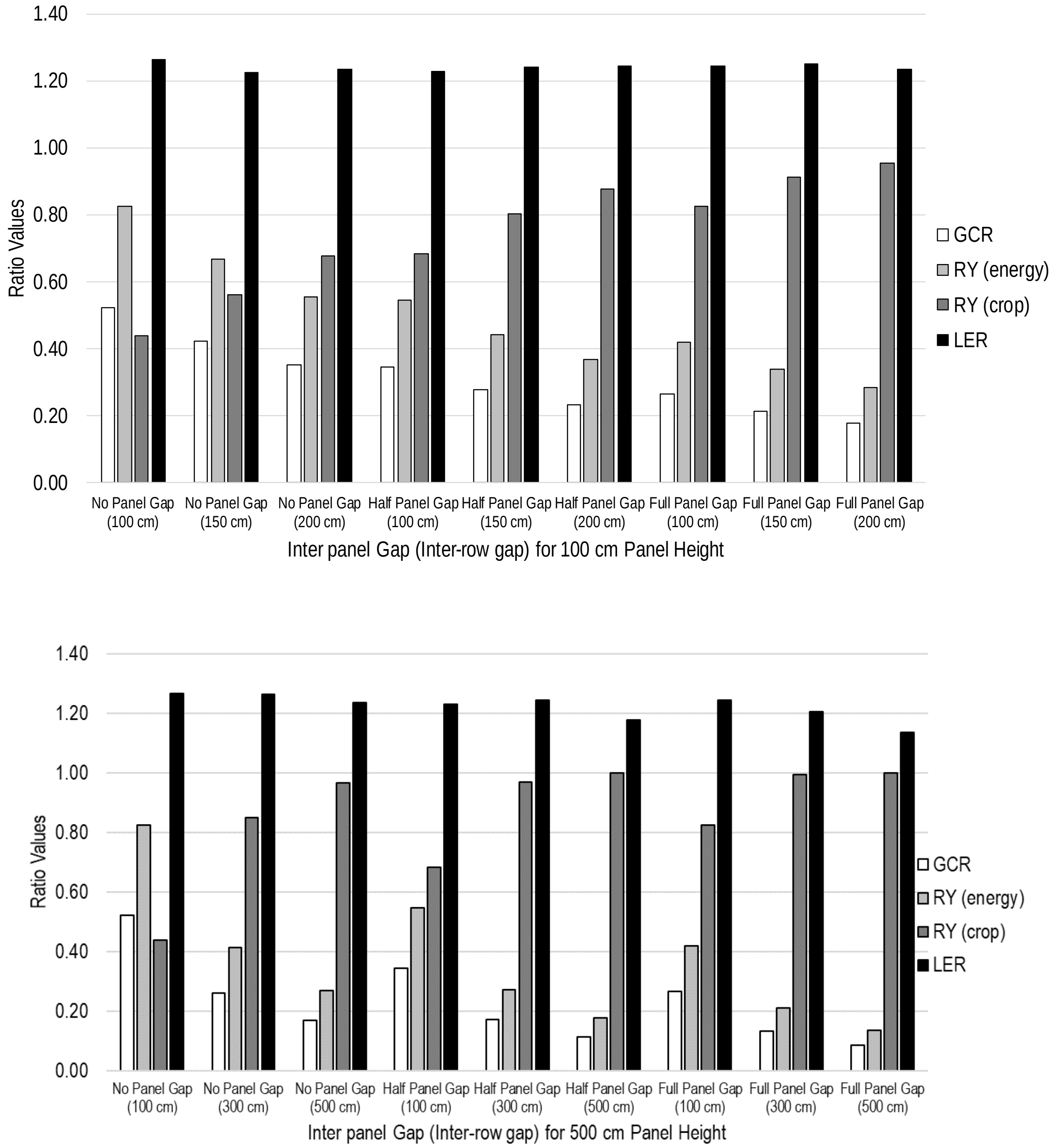

Fig. 4.22 (b). GCR, relative yield (RY) for energy, relative yield (RY) for crop and Land Equivalent Ratio (LER) calculated for different agrivoltaic design parameters considering 100 cm panel height (top) and 500cm panel height (bottom).

4.5 Economic Analysis

4.5.1 Annual Revenue

Here, CAPEX is known as “Capital Expenditure” of the system, which means the total initial investment for installing the system in the very beginning of the project. Normally CAPEX is being spent on the very first year of the project starting. This CAPEX contains all the costs related to the project and some upcoming future costs. As it is an agrivoltaic system focusing on the PV generation, the CAPEX will mostly be related to the system size that has been designed for implementation. Whenever the system size is smaller the CAPEX will also be smaller and for the larger system size the CAPEX will be higher. That's because if the system size is larger that means more panels will be installed and larger inverters will be needed.

Table 4.3.: Parameter considered for CAPEX-OPEX calculation for Energy

Category	**Description**	**Cost per Unit**	**Unit**
Solar Panels	Panel cost per watt	45	BDT/W
Inverter	Inverter cost per kW	4000	BDT/kW
Mounting Structure	Structure cost per panel	1850	BDT/panel
Cabling & Wiring	Cost per kW	2820	BDT/kW
Installation	Installation cost per kW	6670	BDT/kW
Transportation	Transport cost per panel	200	BDT/panel
Miscellaneous	Other fixed costs	120000	BDT
Contingency	Contingency (% of CAPEX)	5	Rate (%)
O&M Cost	Annual O&M (% of CAPEX)	2	Rate (%)
Insurance	Annual Insurance cost	0.5	Rate (%)
Inverter Replacement	Replacement cost after 10 years (% of Inverter Cost)	100	Rate (%)

This table 4.3 shows all the rates and parameters for implementation of the agrivoltaic project. All the rates such as cost per watt for solar panels, electricity selling price are based on Bangladesh's recent market price. All the mounting costs are also based on the Bangladesh rate. The transportation cost per panel is higher because the panel size is larger than usual. The inverter cost will be higher if the system size increases. The total expected system lifetime will be 25 years which is a standard consideration. The annual operation and maintenance (O&M) cost will be combined with annual insurance cost which is in total 2% of the CAPEX. Therefore, inverter replacement costs will be added after 10 years. So, if the system lifetime is 25 years, then inverter replacement cost will take place twice during the project lifetime.

Operational Expenditure (OPEX) for the crops are calculated based on the table 4.4, where possible costing per Hectare land is shown for both Aman and Boro crops. It is evident that Boro requires more cost than Aman.

Table 4.4: Parameter considered for OPEX calculation for crops. [59]

Iteam	Aman Costing (BDT/H.)	Boro Costing (BDT/H)
Fertilizer	7540	9467
Seeding	1375	1375
Plowing	8671	7228
transplanting	7737	7474
Irrigation	8457	17277
Weeding	9342	8457
Pesticide	1893	5114
Harvesting	16342	17571
Processing	1228	3228
Land Charge	9342	9342
Bank Interest	2158	2596

Table 4.5 shows the required parameters to calculate the system payback or Return on Investment (ROI). Here, Inflation Rate, Discount Rate and Loan Interest Rate have been considered as 6%, 8% and 9% respectively.

Table 4.5: Parameter considered for Return on Investment (ROI) or Payback time calculation for the AgriPV system.

Parameter	**Value**	**Unit**	**Description**
Total Panels		pcs	Total number of panels
System Size		KW	Total installed system size
Daily Energy Generation		kWh/day	Daily energy generation
Cost per Watt	45	BDT/W	cost of installing 1 watt of solar panel capacity
Panel Efficiency Degradation	0.8	% per year	Typical annual degradation rate
Electricity Selling Price	7	BDT/kWh	Grid feed-in rate or value of energy
Crop Price Decrease	1	% of CAPEX	Yearly decrease of crop price
System Lifetime	25	Years	Expected lifetime of the system
Inflation Rate	0.06	Rate (6%)	Bangladesh average inflation
Discount Rate	0.08	Rate (8%)	Used for NPV calculations
Loan Interest Rate	0.09	Rate (9%)	Applicable if system is financed
Panel Efficiency	0.19	Rate (19%)	Efficiency of the panels
APV Crop Costing		BDT/ ha	Combine costing for Aman & Boro
APV Crop Revenue		BDT/ ha	Combine revenue for Aman & Boro

The economic analysis indicates a clear trade-off between agricultural and energy revenues as the ground coverage ratio (GCR) increases. With higher GCR values, crop-related profit declines due to increased shading and reduced available solar radiation at the ground level. In contrast, energy-related profit increases almost linearly with GCR, driven by the higher PV capacity per unit land area installed. Fig. 4.24 shows the GCR vs annual profit calculated for different designs considering first year energy profit (top) and crops profit (bottom).

Across all evaluated design configurations, revenue from electricity generation constitutes the dominant share of total system income, accounting for more than 90% of overall profit. As a result, variations in crop revenue have a relatively limited influence on the total agrivoltaic system profitability. This highlights the strong economic dependence of agrivoltaic systems on energy production under current pricing and cost structures.

However, from an agricultural sustainability perspective, excessive increases in GCR are not desirable. The results show that crop profit decreases by more than 50% as GCR increases from 0.10 to 0.50, indicating a substantial reduction in agricultural production under dense PV coverage. Fig. 4.23 shows the shaded region in the plot of first year crops profit (bottom). To limit crop production and profit losses to an acceptable threshold of approximately 25%, the analysis suggests that the GCR should be restricted to a maximum value of 0.30. This value represents a practical compromise between maximizing energy revenue and preserving a reasonable level of agricultural output.

In addition to the effect of GCR, the analysis of inter-row and inter-panel spacing further reinforces the dominant role of energy generation in determining overall system revenue. Increasing inter-row distance or inter-panel gap directly reduces the number of PV modules that can be installed within a given land area, leading to a corresponding decline in installed capacity and annual energy yield. Although wider spacing improves light availability for crops and partially recovers agricultural output, the resulting increase in crop revenue is not sufficient

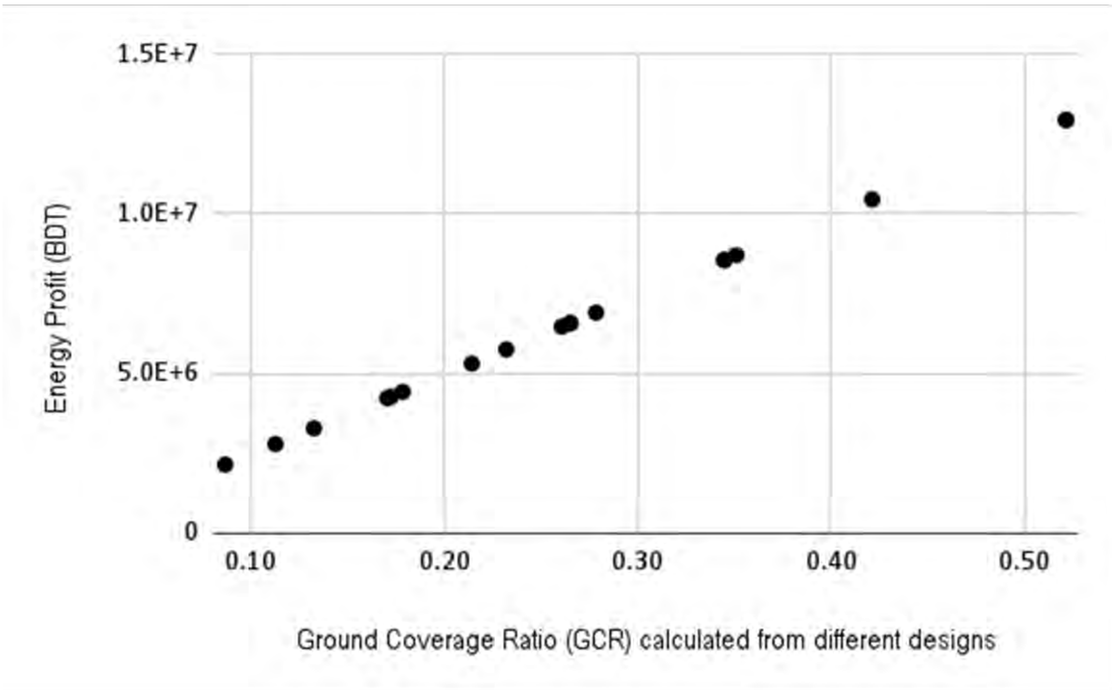

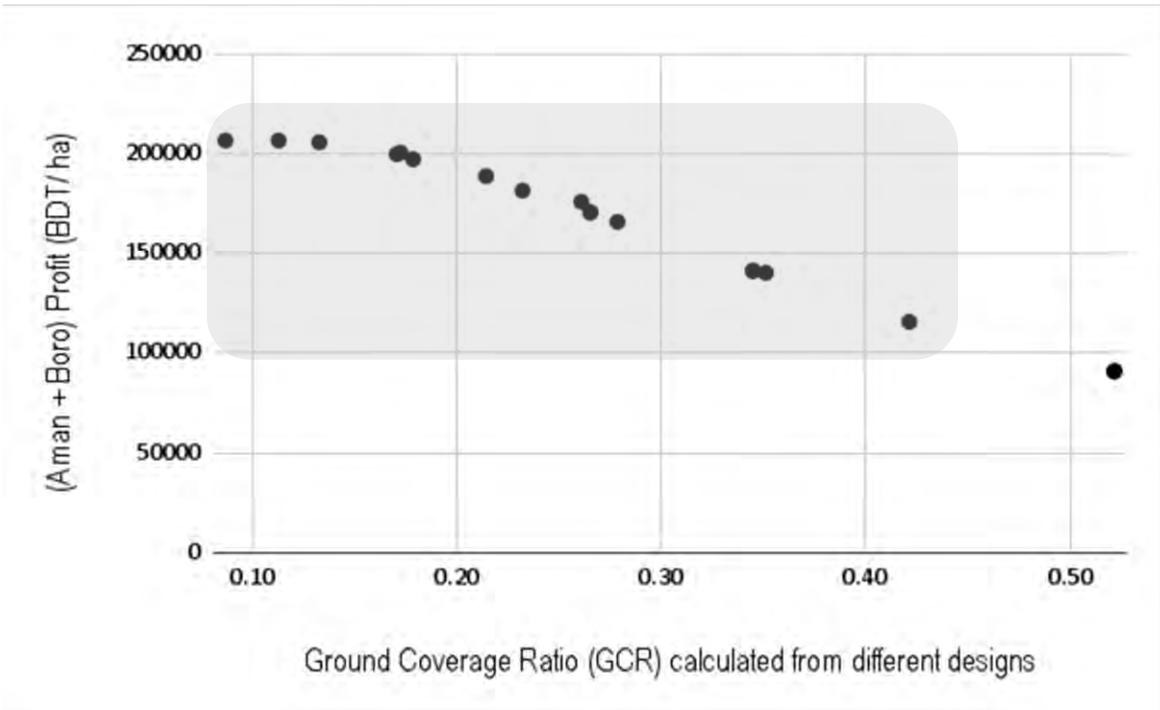

Fig. 4.23. GCR vs annual profit calculated for different designs considering first year energy profit (top) and crops profit (bottom).

to offset the loss in energy income. Consequently, the combined revenue from energy and crops decreases as spacing becomes larger.

This behavior clearly indicates that, under the evaluated economic assumptions, crop revenue contributes a relatively minor share to the total agrivoltaic income compared to electricity sales. Even when crop yield improves due to reduced shading, the financial benefit remains marginal relative to the revenue loss caused by reduced PV density. These findings further support the conclusion that agrivoltaic system optimization in Bangladesh is primarily driven by energy economics, while agricultural considerations act mainly as constraints to limit excessive yield loss rather than as major contributors to total revenue. Fig. 4.24 shows the first-year total revenue calculated for Crops and energy for different design parameters considering 100 cm panel height (top) and 500 cm panel height (bottom). In both cases, total revenue decreases with the increased inter-row gap and inter-panel gap.

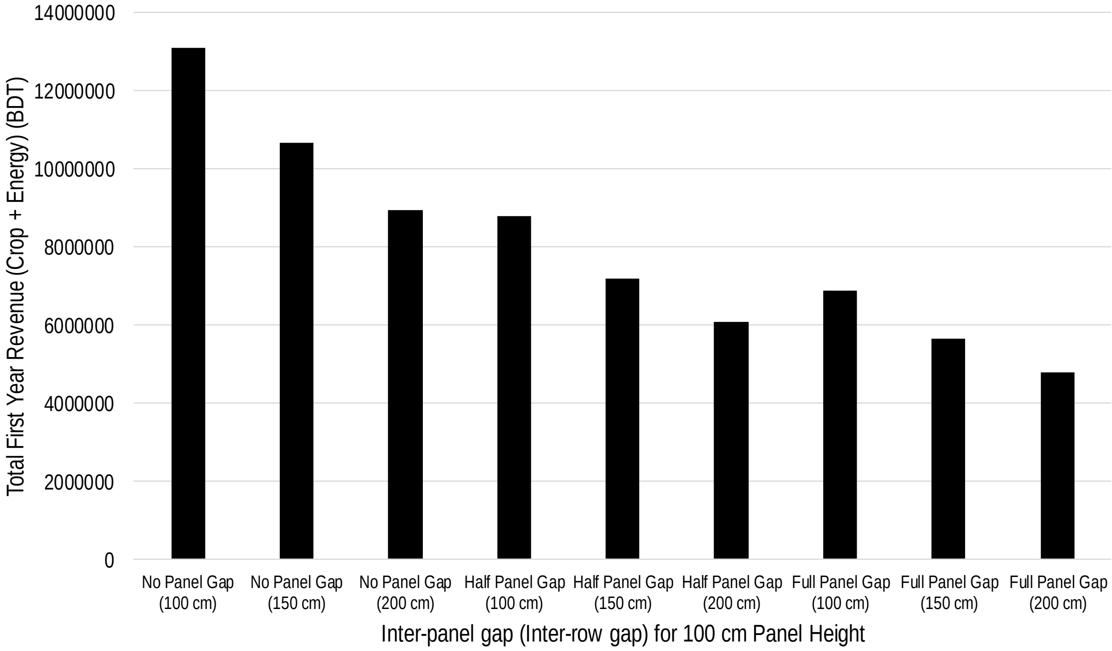

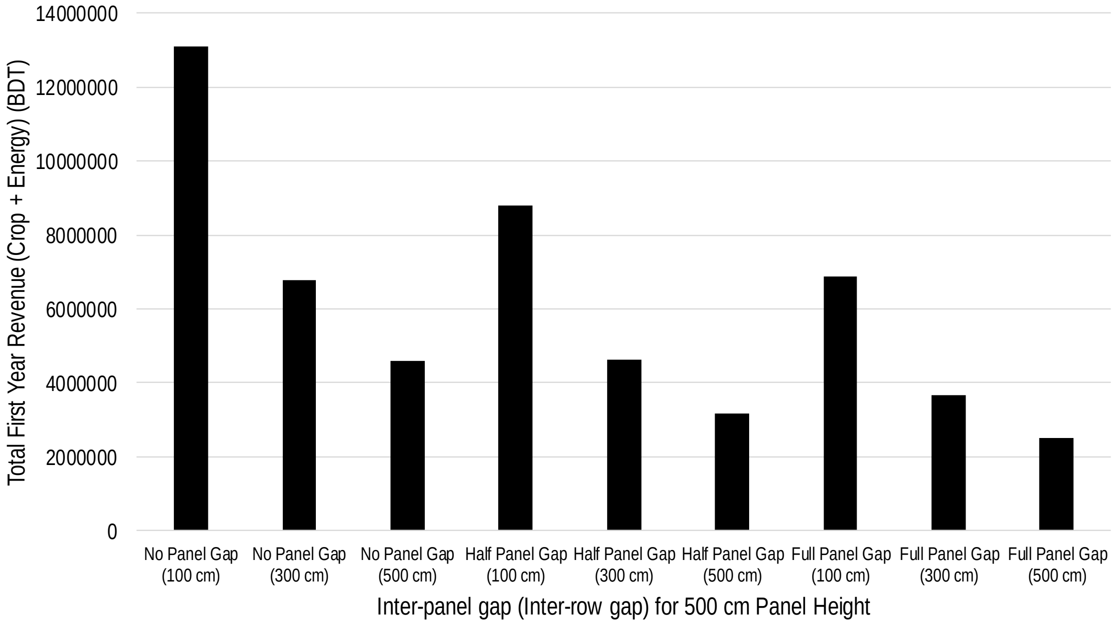

Fig. 4.24. First year total revenue calculated for Crops and energy for different design parameter considering 100 cm panel height (top) and 500 cm panel height (bottom).

4.5.2 Return on Investment (ROI):

Return on Investment signifies the payback time of the studied systems if being integrated. In this study, it is observed that the system considered with different GCR has correlation with the ROI. Fig. 4.25 shows that the GCR is logarithmically related to ROI or payback period. Though the relationship between GCR and ROI is non-linear, however, the fluctuation varies in a smaller range which depicts negligible change occurs in terms of payback period for the considered designs with two seasonal rice crops land considered in this study. It means whether the system parameter changes, overall impact on the payback period varies within months, not in year.

It is evident that, after GCR values 0.30, the change in payback period starts to be saturated. In that case, the closest values of 0.30 GCR could be taken as preferred design from the designs studied. The study suggests keeping Inter-row distance in between 100-300 cm. For small inter-row gap (100-150 cm), the inter-panel gap could be half- or full-length panel gap. For inter-row gap 200 cm or above, no Inter-panel distance is required. Table 6 shows the designs that

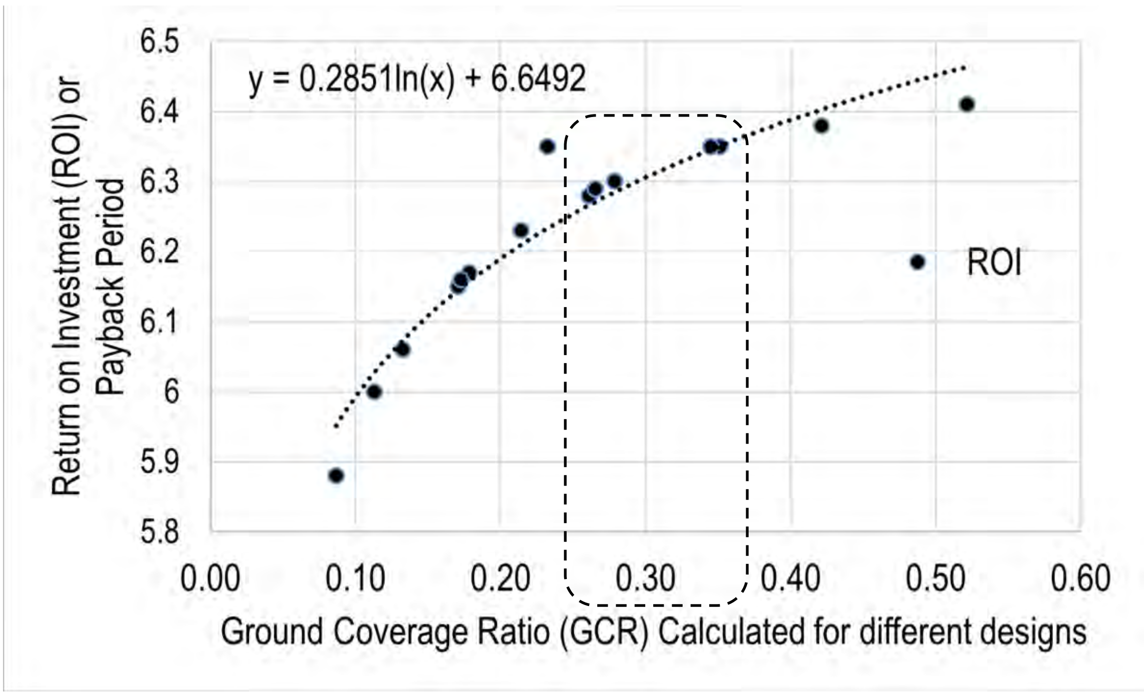

Fig. 4.25. Return on Investment or Payback time calculated for different design considered.

are close to GCR value 0.30 in bold font. It is evident that return on investment does not vary that much (6.15~6.38 years).

Table 4.6: Designs that could be preferable for the selected crops and site (bold).

Panel Height (cm)	Inter-row Gap (cm)	Inter-panel Gap	GCR	ROI
100	100	No Panel Gap	0.52	6.41
		Half Panel Gap	**0.34**	**6.38**
		Full Panel Gap	**0.27**	**6.35**
	150	No Panel Gap	0.42	6.35
		Half Panel Gap	**0.28**	**6.3**
		Full Panel Gap	0.21	6.35
	200	**No Panel Gap**	**0.35**	**6.29**
		Half Panel Gap	0.23	6.23
		Full Panel Gap	0.18	6.17
500	100	No Panel Gap	0.52	6.41
		Half Panel Gap	**0.34**	**6.28**
		Full Panel Gap	**0.27**	**6.15**
	300	**No Panel Gap**	**0.26**	**6.35**
		Half Panel Gap	0.17	6.16
		Full Panel Gap	0.13	6
	500	No Panel Gap	0.17	6.29
		Half Panel Gap	0.11	6.06
		Full Panel Gap	0.09	5.88

Chapter 5

Conclusions and Future Work

5.1 Conclusions

This study presents a comprehensive techno-economic assessment of an agrivoltaic system tailored to the agro-climatic and land-use context of Bangladesh. The study integrates analytical geometric shadow modeling with three-dimensional (3D) shading simulation to evaluate photovoltaic (PV) performance, crop productivity, and overall land-use efficiency under shared land operation. By allowing a conservative upper bound of 25% crop yield reduction for Aman and Boro rice crops, the work establishes a balanced design framework that prioritizes energy generation without significantly compromising agricultural output.

The analysis confirms that fixed-tilt PV installations oriented at an angle equal to the local latitude are more suitable for agrivoltaic deployment in Bangladesh than flat-mounted systems. When seasonal weather conditions, including monsoon-induced cloudy and rainy days, are accounted for, the latitude-tilted configuration yields approximately 11% higher annual incident solar energy.

Seasonal shadow behavior analysis reveals a distinct U-shaped annual pattern, with shadow lengths peaking during the winter months (October to February) due to lower solar elevation angles and reaching minimum values during summer. The study further demonstrates that increasing PV mounting height significantly increases shadow distance across all seasons, thereby mitigating shading impacts on crops during critical growth periods. These findings highlight mounting height as a key design variable for controlling crop exposure while maintaining PV productivity.

A major methodological contribution of this work is the validation of simplified geometric shadow calculations against detailed 3D SketchUp-based simulations. The results show strong agreement between the two approaches, with deviations remaining below 10% across all evaluated scenarios. This confirms that the proposed geometric method, grounded in established solar irradiation models, can reliably approximate shading behavior while substantially reducing computational complexity and design effort.

The trade-off between PV density and agricultural productivity is further examined through variation of inter-row spacing at fixed panel heights. Increasing the inter-row gap leads to a linear reduction in ground coverage ratio (GCR) and energy yield, while simultaneously improving crop yield due to reduced shading. However, for two-crop systems, the land equivalent ratio (LER) remains nearly constant across a wide range of inter-row values, indicating that total land-use efficiency is preserved despite internal redistribution between energy and crop yields.

The results demonstrate that well-designed agrivoltaic configurations can simultaneously sustain crop productivity and enhance solar energy generation, achieving Land Equivalent Ratio (LER) values greater than unity across most design scenarios. Such outcomes indicate a clear advantage over conventional single-use land systems, making agrivoltaics a viable strategy for land-scarce regions of Bangladesh. As a result, this work serves not only as an academic contribution but also as a practical design reference for policymakers, engineers, and agricultural planners seeking scalable agrivoltaic solutions to improve energy security while preserving food production in Bangladesh.

From an economic perspective, the assessment demonstrates that energy revenue overwhelmingly dominates the financial performance of agrivoltaic systems in Bangladesh, contributing more than 90% of total system profit for different design. Based on combined energy yield, crop performance, and profitability analysis, the study recommends an optimal design envelope characterized by a GCR ranging in between 0.25~0.35 and inter-row spacing in the range of 100–300 cm. Additionally, the results indicate that for row spacing of 200 cm or more, no additional inter-panel gap is required, as profit loss remains within the acceptable 25% threshold.

Overall, this research provides a practical, analytically validated, and economically grounded design guideline for agrivoltaic systems in Bangladesh. By demonstrating that simplified geometric shading models can effectively support agrivoltaic design without compromising accuracy, the study contributes toward scalable and locally adaptable agrivoltaic deployment strategies that enhance renewable energy generation while sustaining agricultural productivity in Bangladesh.

5.2 Limitations and Future Work

Despite providing a comprehensive techno-economic framework for agrivoltaic system design in the context of Bangladesh, this study is subject to several limitations that also identify clear directions for future research. First, the PV configuration considered in this work is limited to a fixed-tilt, mono-facial module arrangement with the tilt angle set equal to the local latitude. Future studies may extend the present analysis to include seasonally adjustable tilt, dynamic tilt optimization, or single axis tracking systems. Second, the scope of this study is restricted to conventional mono-facial PV modules arranged in horizontal rows. Emerging agrivoltaic concepts such as bifacial PV modules, vertical or east–west oriented arrays, and elevated panel geometries were not examined. Third, the agricultural assessment in this study is based on a limited set of crop assumptions and does not account for crop-to-crop variability in light tolerance, canopy structure, or seasonal growth behavior. While the selected crops are representative of common agricultural practices in Bangladesh, future research should expand the framework to include a wider range of crop types, including shade-tolerant vegetables, pulses, and high-value horticultural crops.

Future research may explore the integration of higher-capacity photovoltaic (PV) modules with improved conversion efficiencies, which could result in more favorable techno-economic performance of agrivoltaic systems. In addition, incorporating advanced crop–light interaction models and detailed microclimate simulations would enable a more comprehensive assessment of crop response under PV structures, thereby improving the accuracy and robustness of agrivoltaic performance evaluations.

Finally, crop yield response in this study is represented using simplified linear yield reduction assumptions based on shading fraction. This approach does not explicitly model crop physiological responses to light availability, such as photosynthetically active radiation (PAR) utilization, growth-stage-specific sensitivity, or adaptive responses to diffuse radiation. Future research should integrate crop growth and physiological models that account for PAR response curves and critical phenological stages, enabling more accurate estimation of yield under partial shading conditions.

In summary, while the present study establishes a validated design methodology for agrivoltaic systems in Bangladesh, addressing these limitations through advanced PV configurations, diversified crop selection, experimental validation, and crop-specific modeling will significantly enhance the robustness and applicability of future agrivoltaic research

References

[1] A. Ali Abaker Omer et al., “Water evaporation reduction by the agrivoltaic systems development,” Solar Energy, vol. 247, pp. 13–23, Nov. 2022.

[2] W. Liu, A. A. A. Omer, and M. Li, “Agrivoltaic: Challenge and Progress,” Agronomy, vol. 13, no. 7, p. 1934, Jul. 2023.

[3] A. E. Coşgun, “The potential of Agrivoltaic systems in Turkey,” Energy Reports, 2021,vol. 7, pp. 105–111.

[4] S. Schindele et al., “Implementation of agrophotovoltaics: Technoeconomic analysis of the price-performance ratio and its policy implications,” Applied Energy, vol. 265, p. 114737, May 2020.

[5] H. Jo et al., “Comparison of Yield and Yield Components of Several Crops Grown under Agro-Photovoltaic System in Korea,” Agriculture, vol. 12, no. 5, p. 619, Apr. 2022.

[6] G. P. Moreda, M. A. Muñoz, Montserrat Alonso-Garcia, and L. Hernández-Callejo, “Techno-Economic Viability of AgroPhotovoltaic Irrigated Arable Lands in the EU-Med Region: A Case- Study in Southwestern Spain,” vol. 11, no. 3, pp. 593–593, Mar. 2021.

[7] Y. Sasaki, T. Itabashi, T. Hamada and N. Koshizuka, "Forecasting Insolation Shaded by Solar Panels for Optimal Layout in Agrivoltaic System," 2023 IEEE 12th Global Conference on Consumer Electronics (GCCE), Nara, Japan, 2023.

[8] N.F. Othman, M.E. Ya'acob, A.S. Abdul-Rahim, Mohd Shahwahid Othman, M.A.M. Radzi, H. Hizam, Y.D. Wang, A.M. Ya'acob, H.Z.E. Jaafar, “Embracing new agriculture

commodity through integration of java tea as high value herbal crops in solar pv farms", Journal of Cleaner Production,ELSVIER},Volume 91, Pages 71-77,15 March 2015.

[9] Elnaz Hassanpour Adeh ,John S. Selker,Chad W. Higgins,``Remarkable agrivoltaic influence on soil moisture, micrometeorology and water-use efficiency", November 1,2018.

[10] C. Amaducci, E. Yin, and M. Colauzzi, "Agrivoltaic systems to optimize land use for electric energy production," Applied Energy, vol. 220, pp. 545–561, 2018 [6]

[11] H. Dinesh and J. M. Pearce, "The potential of agrivoltaic systems," Renewable and Sustainable Energy Reviews, vol. 54, pp. 299–308, 2016.

[12] GOETZBERGER, A., & ZASTROW, A. (1982). On the Coexistence of Solar-Energy Conversion and Plant Cultivation. *International Journal of Solar Energy*, *1*(1), 55–69.

[13] C. Dupraz, H. Marrou, G. Talbot, L. Dufour, A. Nogier, Y. Ferard (2011). Combining solar photovoltaic panels and food crops for optimising land use: Towards new agrivoltaic schemes, Renewable Energy, Volume 36, Issue 10, Pages 2725-2732, ISSN 0960-1481

[14] H. Marrou, L. Guilioni, L. Dufour, C. Dupraz, J. Wery (2013). Microclimate under agrivoltaic systems: Is crop growth rate affected in the partial shade of solar panels?, Agricultural and Forest Meteorology, Volume 177, Pages 117-132, ISSN 0168-1923,

[15] Harshavardhan Dinesh, Joshua M. Pearce (2016). The potential of agrivoltaic systems, Renewable and Sustainable Energy Reviews, Volume 54, Pages 299-308, ISSN 1364-0321

[16] Schindele, S.; Trommsdorff, M.; Schlaak, A.; Obergfell, T.; Bopp, G.; Reise, C.; Braun, C.; Weselek, A.; Bauerle, A.; Högy, P.; et al. Implementation of Agrophotovoltaics: Techno-Economic Analysis of the Price-Performance Ratio and Its Policy Implications. *Appl. Energy* **2020**, *265*, 114737.

[17] Lee, S., Lee, J., Jeong, Y., Kim, D., Seo, B., Seo, Y., Kim, T., & Choi, W. (2023). Agrivoltaic system designing for sustainability and smart farming: Agronomic aspects and design criteria with safety assessment. *Applied Energy*, *341*, 121130

[18] Trommsdorff, M., Vorast, M., Durga, N., & Padwardhan, S. M. (2021). Potential of agrivoltaics to contribute to socio-economic sustainability: A case study in Maharashtra/India. *AIP Conference Proceedings*.

[19] Elkadeem, M. R., Zainali, S., Lu, S. M., Younes, A., Abido, M. A., Amaducci, S., Croci, M., Zhang, J., Landelius, T., Stridh, B., & Campana, P. E. (2023). Agrivoltaic systems potentials in Sweden: A geospatial-assisted multi-criteria analysis. *Applied Energy*, *356*, 122108

[20] Chalgynbayeva, A., Balogh, P., Szőllősi, L., Gabnai, Z., Apáti, F., Sipos, M., & Bai, A. (2024). The Economic Potential of Agrivoltaic Systems in Apple Cultivation—A Hungarian Case Study. *Sustainability*, *16*(6), 2325

[21] Seck, P. A., Diagne, A., Mohanty, S., & Wopereis, M. C. S. (2012b). Crops that feed the world 7: Rice. *Food Security*, *4*(1), 7–24

[22] Thum, C. H., Okada, K., Yamasaki, Y., & Kato, Y. (2025). Impacts of agrivoltaic systems on microclimate, grain yield, and quality of lowland rice under a temperate climate. *Field Crops Research*, *326*, 109877

[23] Chatzipanagi, A., Taylor, N., & Jaeger-Waldau, A. (2023). Overview of the potential and challenges for Agri-Photovoltaics in the European Union. *JRC Publications Repository*

[24] Sultan Tekie, Sebastian Zainali, Tekai Eddine Khalil Zidane, Silvia Ma Lu, Mohammed Guezgouz, Jie Zhang, Stefano Amaducci, Christian Dupraz, Pietro Elia Campana, Unraveling the crop yield response under shading conditions through the deployment of a drought index: A meta-analysis, Energy Nexus, Volume 19, 2025, 100523,

[25] Sekiyama, T., & Nagashima, A. (2019b). Solar sharing for both food and clean energy production: performance of agrivoltaic systems for corn, a typical Shade-Intolerant crop. *Environments*, *6*(6), 65.

[26] Mead, R., & Willey, R. W. (1980). The Concept of a 'Land Equivalent Ratio' and Advantages in Yields from Intercropping. *Experimental Agriculture*, *16*(3), 217–228.

[27] Barron-Gafford, G. A., Pavao-Zuckerman, M. A., Minor, R. L., Sutter, L. F., Barnett-Moreno, I., Blackett, D. T., Thompson, M., Dimond, K., Gerlak, A. K., Nabhan, G. P., & Macknick, J. E. (2019). Agrivoltaics provide mutual benefits across the food–energy–water nexus in drylands. *Nature Sustainability*, *2*(9), 848–855.

[28] Valle, B., Simonneau, T., Sourd, F., Pechier, P., Hamard, P., Frisson, T., Ryckewaert, M., & Christophe, A. (2017). Increasing the total productivity of a land by combining mobile photovoltaic panels and food crops. *Applied Energy*, *206*, 1495–1507

[29] Hermelink, M. I., Maestrini, B., & De Ruijter, F. J. (2024). Berry shade tolerance for agrivoltaics systems: A meta-analysis. *Scientia Horticulturae*, *330*, 113062

[30] Trommsdorff, M., Kang, J., Reise, C., Schindele, S., Bopp, G., Ehmann, A., Weselek, A., Högy, P., & Obergfell, T. (2021). Combining food and energy production: Design of an

agrivoltaic system applied in arable and vegetable farming in Germany. *Renewable and Sustainable Energy Reviews*, *140*, 110694

[31] Campana, P. E., Stridh, B., Amaducci, S., & Colauzzi, M. (2021b). Optimisation of vertically mounted agrivoltaic systems. *Journal of Cleaner Production*, *325*, 129091

[32] Touil, S., Richa, A., Fizir, M., & Bingwa, B. (2021). Shading effect of photovoltaic panels on horticulture crops production: a mini review. *Reviews in Environmental Science and Bio/Technology*, *20*(2), 281–296.

[33] H. M. Fahad, A. Islam, M. Islam, M. F. Hasan, W. F. Brishty and M. M. Rahman, "Comparative Analysis of Dual and Single Axis Solar Tracking System Considering Cloud Cover," *2019 International Conference on Energy and Power Engineering (ICEPE)*, Dhaka, Bangladesh, 2019, pp. 1-5

[34] Roger A Messenger and Jerry Ventre., *Photovoltaic Systems Engineering.*, 2nd Edition. CRC Press LLC, 2004

[35] Wenham, Stuart & Green, Martin & Watt, Muriel & Corkish, Richard. , “Applied photovoltaics,” second edition, 2013.

[36] J. Weselek et al., "Agrivoltaic systems: Applications, challenges, and opportunities. A review," *Renewable and Sustainable Energy Reviews*, vol. 144, 2021.

[37] A. Elamri, H. Cheviron, C. Lopez, G. Dejean, and M. Belaud, "Water budget and crop modelling for agrivoltaic systems: Application to irrigated lettuces," Agricultural Water Management, vol. 208, pp. 440–453, 2018

[38] M. Trommsdorff, M. Kang, D. Reise, and J. Schindele, "Combining food and energy production: Design of an agrivoltaic system applied in arid regions," Agrosyst. Geosci. Environ., vol. 2, no. 1, 2019

[39] J. Weselek et al., "Agrivoltaic systems: Applications, challenges, and opportunities. A review," *Renewable and Sustainable Energy Reviews*, vol. 144, 2021

[40] M. Aroca-Delgado, A. Fernández-García, P. López-Luque, and E. Pérez-Higueras, "Optimization of yield production in solar greenhouses by shading with photovoltaic panels," *Renewable Energy*, vol. 113, pp. 63–77, 2017

[41] M. A. Green, "Solar cell efficiency tables (version 58)," Prog. Photovolt: Res. Appl., vol. 29, pp. 3–15, 2021.

[42] A. Riaz et al., "Agrivoltaics: A climate-smart approach for food and energy production in South Asia," *Renewable Energy*, vol. 187, pp. 451–466, 2022

[43] T. Min et al., "A comprehensive evaluation of shading impacts on photovoltaic arrays using simulation models," *Energy Reports*, vol. 6, pp. 446–453, 2020

[44] A. Elamri et al., "Water budget and crop modelling for agrivoltaic systems: Application to irrigated lettuces," *Agricultural Water Management*, vol. 208, pp. 440–453, 2018

[45] H. Dinesh and J. M. Pearce, "The potential of agrivoltaic systems," *Renewable and Sustainable Energy Reviews*, vol. 54, pp. 299–308, 2016

[46] D. Majumdar and M. Pasqualetti, "Dual use of agricultural land: Introducing 'agrivoltaics' in Phoenix Metropolitan Statistical Area, USA," *Land Use Policy*, vol. 95, 2020.

[47] Renewable Power Generation Costs in 2020 (IRENA 2021).

[48] NREL System Advisor Model (SAM) O&M cost modeling (Gilman et al., *SAM Documentation*).

[49] IEC 61215/61724 (PV panel performance degradation guidance), and NREL technical reports on PV degradation

[50] NREL SAM revenue & degradation modeling; IEA PVPS financial modules

[51] Agricultural economics models for dual-use systems (e.g., agrivoltaics studies in *Renewable Energy* and *Agroforestry Systems* journals); standard farm budgeting methods (USDA or FAO extension publications).

[52] IEA-PVPS Task 13 (2025). *Dual Land Use for Agriculture and Solar Power Production*.

[53] Gallo, A., & Mingozzi, A. (2019). Discounted Cash Flow (DCF) Methodologies in Energy Projects. Energy Procedia, 159, 58–63.

[54] Standard NPV formula from financial economics and renewable energy project evaluation (IRENA, NREL SAM documentation).

[55] Capital budgeting literature (e.g., Brealey & Myers, Principles of Corporate Finance) or IEA/IRENA financial manuals.

[56] Hwang, K. W., et al. (2024). Estimating the Deterministic and Stochastic LCOE of Agrivoltaics. Applied Energy, 366, 122158

[57] Financial project evaluation literature (e.g., IEA, NREL, or textbook coverage in Renewable Energy Finance).

[58] J. Appelbaum, and J. Bany. "Shadow effect of adjacent solar collectors in large scale systems." Solar Energy, vol. 23.6, pp.497-507, 1979.

[59] Chanda, S. C., Ali, M. A., Haque, M. E., Abdullah, M. R. and Sarwar, A. K. M. G. (2019). Cost of production and cost benefit analysis of different rice in Sirajganj district. Asian Journal of Crop, Soil Science and Plant Nutrition, 01(01), 07-14.

[60] R. S. Gonocruz, T. Maraseni, and Y. Egawa, "Analysis of the rice yield under an agrivoltaic system: A case study in Japan," Environments, vol. 8, no. 3, p. 25, 2021, doi: 10.3390/environments8030025

[61] C.-H. Thum, T. Nakaji, and Y. Watanabe, "Impacts of agrivoltaic systems on microclimate, grain yield, and quality of lowland rice under a temperate climate," Field Crops Research, vol. 315, p. 109135, 2025,

[62] S. Yun, H. Min, and J. Park, "Assessment of rice productivity and solar power generation in agriphotovoltaic systems," Agriculture, vol. 15, no. 1, p. 17, 2025

[63] J. Park, H. Min, Y. Jeong, and S. Yun, "Rice yield and electricity production in agro-photovoltaic systems," Chilean Journal of Agricultural Research, vol. 84, no. 2, pp. 131–141, 2024,

[64] H. Jo, G. Lee, T. Kim, and E. Lee, "Evaluation of yield and yield components of rice in vertical agro-photovoltaic system in South Korea," Agriculture, vol. 14, no. 6, p. 920, 2024

[65] R. Nasukawa, Y. Yamashita, and M. Honda, “Rice yield and energy balance in an agrivoltaic system under insufficient light and heavy shading conditions,” Science of the Total Environment, vol. 969, p. 173702, 2025,

[66] M. Kim, S. Lee, K. Kim, and Y. Hwang, “Integrated assessment framework for rice yield and energy yield in bifacial agrivoltaic systems,” Energies, vol. 17, no. 3, p. 464, 2024

[67] X. Jia, H. Wang, B. Liu, and Y. Liang, “Variations of solar radiation and their impact on rice growth under agrivoltaic systems,” Preprints, pp. 1–17, 2025

[68] C.-H. Thum, “Simulation Approach to Estimate Rice Yield and Energy Generation under Agrivoltaic System,” M.S. thesis, The University of Tokyo, Tokyo, Japan, 2019.

[69] Y. Okada et al., “Case-study of rice farming in Japan under agriphotovoltaic system,” Journal of Photonics for Energy, vol. 15, no. 3, p. 032704, 2025,

[70] C. Dupraz et al., “Assessment of the ground coverage ratio of agrivoltaic systems as a proxy for potential crop productivity,” Agroforestry Systems, vol. 97, pp. 225–242, 2023,

[71] Zainali, S., Ma Lu, S., et al., Modelling, simulation, and optimisation of agrivoltaic systems: a comprehensive review, Applied Energy, 2025

[72] Al-Amin, *et al.*"Agrivoltaics system for sustainable agriculture and green energy in Bangladesh", Appl. Energy, vol. 371, 2024.

[73] Agrivoltaics: A Sustainable Path to Food and Energy Security of Bangladesh, Light Castle Analytics Wing, August 5, 2025

[74] Article available online: https://www.pv-magazine.com/2024/07/26/researchers-find-agrivoltaics-have-lcoe-of-0-039-kwh-7-year-payback-time-in-india/

[75] Agrivoltaics in India: Challenges and opportunities for scale-up, IISD REPORT

[76] Yoo, S.; Lee, K. Integrated Assessment Framework for Rice Yield and Energy Yield in Bifacial Agrivoltaic Systems. Energies, vol.18, No. 6359, 2025.

[77] N. Giri, S.Poonia, R. Mohanty, M. Bajaj, R. Nath, & Y. Belkhier, "Agriphotovoltaic System to Improve Land Productivity and Revenue of Farmer", 2022.

Appendix A. Sample Calculator

Energy Calculation

Parameter	Value	Unit	Description
Total Panels	510	pcs	Total number of panels
System Size	168.3	KW	Total installed system size
Daily Energy Generation	841.5	kWh/day	Daily energy generation
Cost per Watt	45	BDT/W	cost of installing 1 watt of solar panel capacity
Panel Efficiency Degradation	0.8	% per year	Typical annual degradation rate
Electricity Selling Price	7	BDT/kWh	Grid feed-in rate or value of energy
Crop Price Decrease	1	% of CAPEX	Yearly decrease of crop price
System Lifetime	25	Years	Expected lifetime of the system
Inflation Rate	0.06	Rate (6%)	Bangladesh average inflation
Discount Rate	0.08	Rate (8%)	Used for NPV calculations
Loan Interest Rate	0.09	Rate (9%)	Applicable if system is financed
Panel Efficiency	0.19	Rate (19%)	Efficiency of the panels
APV Crop Costing	162996.12	BDT/ ha	Combine costing for Aman & Boro
APV Crop Revenue	369479.38	BDT/ ha	Combine revenue for Aman & Boro
Per Panel Rating (Watt) =	330	User Input	
Total Rows Count =	17	User Input	
Panels Per Row =	30	User Input	
Total Panels =	510		
System Size (KW) =	168.3		
Per Panel area (Sq m2) =	1.7	User Input	
Total Panel Area (Sq m2) =	867		
Daily Electrical Energy (KWh/Day) =	841.5		
Peak Sun Hours (h)	5	User Input	
Annual Generation (KWh/Year) =	307147.50		

CAPEX-OPEX

Category	Description	Cost per Unit	Unit	Quantity	Total Cost (BDT)
Solar Panels	Panel cost per watt	45	BDT/W	168.30	7573500
Inverter	Inverter cost per kW	4000	BDT/kW	168.3	673200
Mounting Structure	Structure cost per panel	1850	BDT/panel	510.00	943500
Cabling & Wiring	Cost per kW	2820	BDT/kW	168.3	474606
Installation	Installation cost per kW	6670	BDT/kW	168.3	1122561
Transportation	Transport cost per panel	200	BDT/panel	510.00	102000
Miscellaneous	Other fixed costs	120000	BDT	1	120000
Total CAPEX	Total calculated CAPEX (Category 2 to 8)	11009367	BDT	1	11009367
Contingency	Contingency (% of CAPEX)	5	Rate (%)	550468.35	550468.35
O&M Cost	Annual O&M (% of CAPEX)	2	Rate (%)	220187.34	220187.34
Insurance	Annual Insurance cost	0.5	Rate (%)	55046.835	55046.835
Inverter Replacement	Replacement cost after 10 years (% of Inverter Cost)	100	Rate (%)	673200	673200
Crop Production Costing	Total Yearly Expenses For Crop Production (HYV)	162996.12	BDT/ ha	1	162996.12
Total CAPEX	12233035.35				
Annual OPEX	438230.29				

Annual Cash Flow

Year	Annual Energy Generation (kWh)	Crop Yield Income (BDT/ha)	Annual Energy Income (BDT)	Total Annual Income (Crop + Energy) (BDT)	O&M Cost (BDT)	Inverter Replacement (BDT)	Net Cash Flow (BDT)	Cumulative Cash Flow (BDT)
1	307147.50	369479.38	2150032.50	2519511.88	438230.29	0	2081281.59	2081281.59
2	304690.32	365784.59	2132832.24	2498616.83	438230.29	0	2060386.54	4141668.13
3	302252.80	362126.75	2115769.58	2477896.33	438230.29	0	2039666.04	6181334.17
4	299834.78	358505.48	2098843.43	2457348.90	438230.29	0	2019118.61	8200452.78
5	297436.10	354920.42	2082052.68	2436973.10	438230.29	0	1998742.81	10199195.59
6	295056.61	351371.22	2065396.26	2416767.48	438230.29	0	1978537.18	12177732.78
7	292696.16	347857.51	2048873.09	2396730.59	438230.29	0	1958500.30	14136233.08
8	290354.59	344378.93	2032482.10	2376861.03	438230.29	0	1938630.74	16074863.82
9	288031.75	340935.14	2016222.25	2357157.39	438230.29	0	1918927.10	17993790.92
10	285727.50	337525.79	2000092.47	2337618.26	438230.29	673200	1226187.97	19219978.88
11	283441.68	334150.53	1984091.73	2318242.26	438230.29	0	1880011.97	21099990.85
12	281174.14	330809.03	1968218.99	2299028.02	438230.29	0	1860797.73	22960788.58
13	278924.75	327500.94	1952473.24	2279974.18	438230.29	0	1841743.89	24802532.47
14	276693.35	324225.93	1936853.46	2261079.38	438230.29	0	1822849.09	26625381.56
15	274479.80	320983.67	1921358.63	2242342.30	438230.29	0	1804112.01	28429493.57
16	272283.97	317773.83	1905987.76	2223761.59	438230.29	0	1785531.30	30215024.87
17	270105.69	314596.09	1890739.86	2205335.95	438230.29	0	1767105.66	31982130.53
18	267944.85	311450.13	1875613.94	2187064.07	438230.29	0	1748833.78	33730964.31
19	265801.29	308335.63	1860609.03	2168944.66	438230.29	0	1730714.37	35461678.67
20	263674.88	305252.27	1845724.15	2150976.43	438230.29	673200	1039546.14	36501224.81
21	261565.48	302199.75	1830958.36	2133158.11	438230.29	0	1694927.82	38196152.63
22	259472.96	299177.75	1816311	2115488.45	438230.29	0	1677258	39873410.79
23	257397.17	296185.98	1801780.21	2097966.19	438230.29	0	1659735.89	41533146.69
24	255338.00	293224.12	1787365.97	2080590.08	438230.29	0	1642359.79	43175506.48
25	253295.29	290291.88	1773067.04	2063358.92	438230.29	0	1625128.62	44800635.10

Appendix B. Calculated Shadow length

	Shadow Length (Sketch Up) (cm)		Shadow Length (MATLAB) (cm)		100 cm Panel Height
	9:00 AM	**12:00 PM**	**9:00 AM**	**12:00 PM**	
15-Jan-24	285	232.6	290	248	
15-Feb-24	223.9	195.7	226	206	
15-Mar-24	165.7	159.5	167	163	
15-Apr-24	118.2	126	120.3	130.2	
15-May-24	88.8	103.3	92.2	105	
15-Jun-24	87.4	93.1	106.6	94.7	
15-Jul-24	88.4	97.4	101.1	99.1	
15-Aug-24	103.8	116.1	105.2	118.7	
15-Sep-24	144.6	144.9	147.6	150.3	
15-Oct-24	193.8	181.1	203.4	188.6	
15-Nov-24	250.1	220.6	270	236	
15-Dec-24	293	243.8	341	260	
	Shadow Length (Sketch Up) (cm)		Shadow Length (MATLAB) (cm)		500 cm Panel Height
	9:00 AM	**12:00 PM**	**9:00 AM**	**12:00 PM**	
15-Jan-24	830.3	630.8	807	666	
15-Feb-24	597.7	490.7	592	521	
15-Mar-24	376.4	353.1	388	373	
15-Apr-24					
15-May-24					
15-Jun-24	87.2	95.6	151	106.2	
15-Jul-24	88.3	113.8	130	123.2	
15-Aug-24	140.9	185.9	145	197.7	
15-Sep-24	296.5	298	307	317.9	
15-Oct-24	483.3	440	535	464.3	
15-Nov-24	697	585.6	776	623	
15-Dec-24	860.5	673.4	876	710	

Appendix C. Crop Yield

Panel Height (cm)	Total Panel + Row Gap (cm)	Row To Row Gap (cm)	Row Count	Panel Configuration	GCR	Relative Yield (Aman)	Relative Yield (Boro)	APV Aman Yield (kg/ ha)	APV Boro Yield (kg/ ha)	Combine Relative Yield (Aman & Boro)
100	191.7	100	52	No Panel Gap	0.52	0.44	0.44	2200.03	2775.65	0.44
				Half Panel Gap	0.34	0.71	0.66	3524.74	4208.96	0.68
				Full Panel Gap	0.27	0.84	0.81	4203.06	5129.39	0.82
100	241.7	150	42	No Panel Gap	0.42	0.58	0.54	2907.76	3423.88	0.56
				Half Panel Gap	0.28	0.82	0.79	4092.14	4980.02	0.80
				Full Panel Gap	0.21	0.92	0.91	4584.36	5739.55	0.91
100	291.7	200	35	No Panel Gap	0.35	0.70	0.66	3492.60	4184.01	0.68
				Half Panel Gap	0.23	0.89	0.87	4449.07	5481.70	0.88
				Full Panel Gap	0.18	0.96	0.95	4795.22	5994.83	0.95
500	191.7	100	52	No Panel Gap	0.52	0.44	0.44	2200.03	2775.65	0.44
				Half Panel Gap	0.34	0.71	0.66	3524.74	4208.96	0.68
				Full Panel Gap	0.27	0.84	0.81	4203.06	5129.39	0.82
500	391.7	300	26	No Panel Gap	0.26	0.85	0.85	4237.97	5385.27	0.85
				Half Panel Gap	0.17	0.97	0.97	4856.40	6113.25	0.97
				Full Panel Gap	0.13	1.00	0.99	4968.34	6284.51	0.99
500	591.7	500	17	No Panel Gap	0.17	0.98	0.96	4864.11	6061.81	0.97
				Half Panel Gap	0.11	1.00	1.00	4968.34	6332.00	1.00
				Full Panel Gap	0.09	1.00	1.00	4968.34	6332.00	1.00